Gamma-ray detection from space: MeV and GeV energies

Jean Ballet
AIM, CEA Saclay
Fermi-LAT collaboration
with Ph. Bruel and Ph. Laurent

ISAPP school June 17, 2026

Outline of the presentation

I. Generalities
II. Background
III. Photoelectric detectors
IV. Compton detectors
V. Pair-production detectors

I. Generalities

Detector types

Gamma rays in the MeV and GeV ranges are **only detectable by detectors in space** because the atmosphere is opaque (the TeV range with the atmosphere as detector was covered by F. Bradascio last Thursday).

- MeV range: **counters** (CGRO/BATSE 1991-2000, **Fermi/GBM 2008**)
- Below 1 MeV: **coded masks** (Integral 2002-2025, **Swift/BAT 2004, SVOM/ECLAIRS 2024**)
- Below 100 MeV: **Compton** detectors (CGRO/COMPTEL 1991-2000, **AMEGO, Astrogam**, **COSI 2029**)
- GeV range: **Pair-production** detectors (CGRO/EGRET 1991-2000, **Fermi/LAT 2008**)

What we want to measure

Gamma rays are detected as individual photons whose characteristics are:

- **Arrival direction**: most important to identify the origin of the signal, challenging in this energy range. **Main topic of this presentation.**
- **Time**: easy to reach **μs** resolution, absolute reference is the main difficulty. Not addressed here.
- **Energy**: easy to reach **< 10%** resolution, good enough for continuous spectra. Specific detectors (like Ge) allow much better resolution (close to **0.1%**) for MeV lines. Not addressed here.
- **Polarisation** (linear): relatively natural with Compton detectors and integrated in future projects, also doable with pair production. In both cases, **poor** phase resolution.

Photon-matter interaction

Plot for **water** (light)

Light materials offer a large range for Compton detection

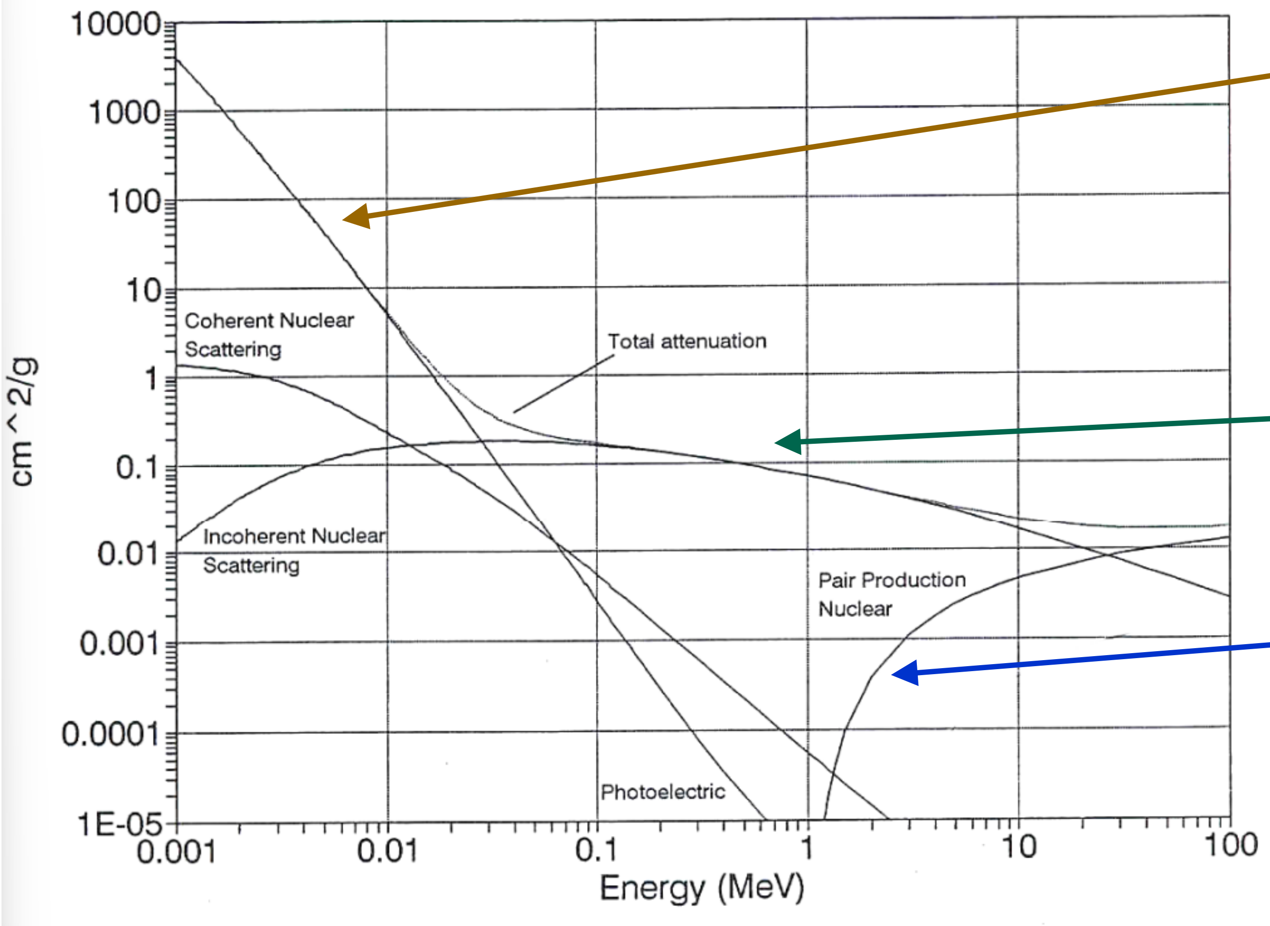

Mass Attenuation Coefficients for Photons in Water

Photoelectric effect at low energies: photon entirely absorbed, ionisation → electron → light and position
Scintillating crystals (NaI, CsI) allow measuring the amount of light → energy

Compton at intermediate energies: photon is deflected and can be redetected, both energies and positions can be measured

Pair creation above 10 MeV: photon entirely transformed into electron and positron → tracking to get direction

Photon-matter interaction

Plot for **lead** (heavy)

Heavier materials reduce the range of the Compton effect

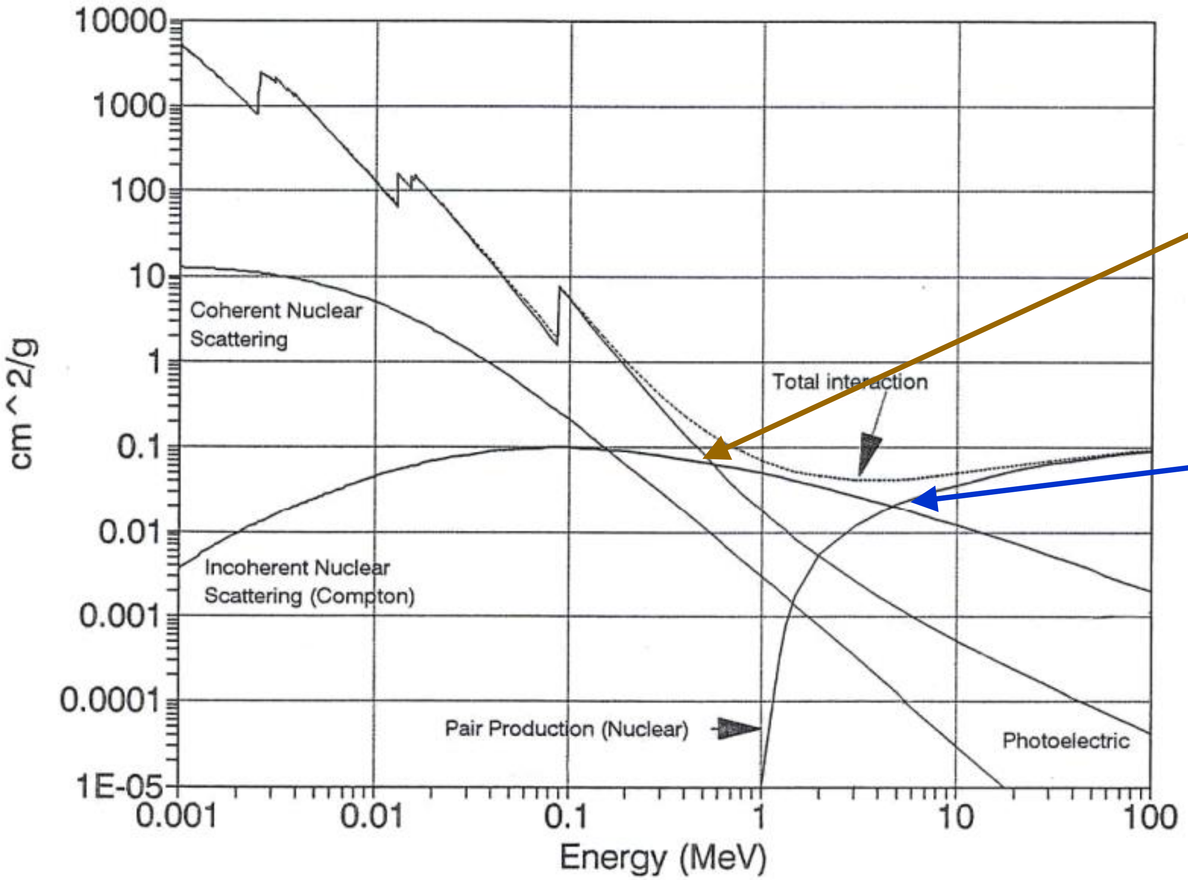

Mass Attenuation Coefficients for Photons in Lead

Transition between **photoelectric** and **Compton** effects between 30 (light) and 500 (heavy) keV

Transition between **Compton** effect and **pair creation** between 5 (heavy) and 30 (light) MeV

II. Background

Particle background

- ✓ The background is, together with the effective area (limited by the size and weight of the instrument), what drives the **detection threshold**.
- ✓ In space the cosmic rays and solar particles create many interactions in the detector
- ✓ Many more charged particles than gamma rays ➔ **strong background**
- ✓ Irradiation has both immediate (background) and delayed (**activation**) effects

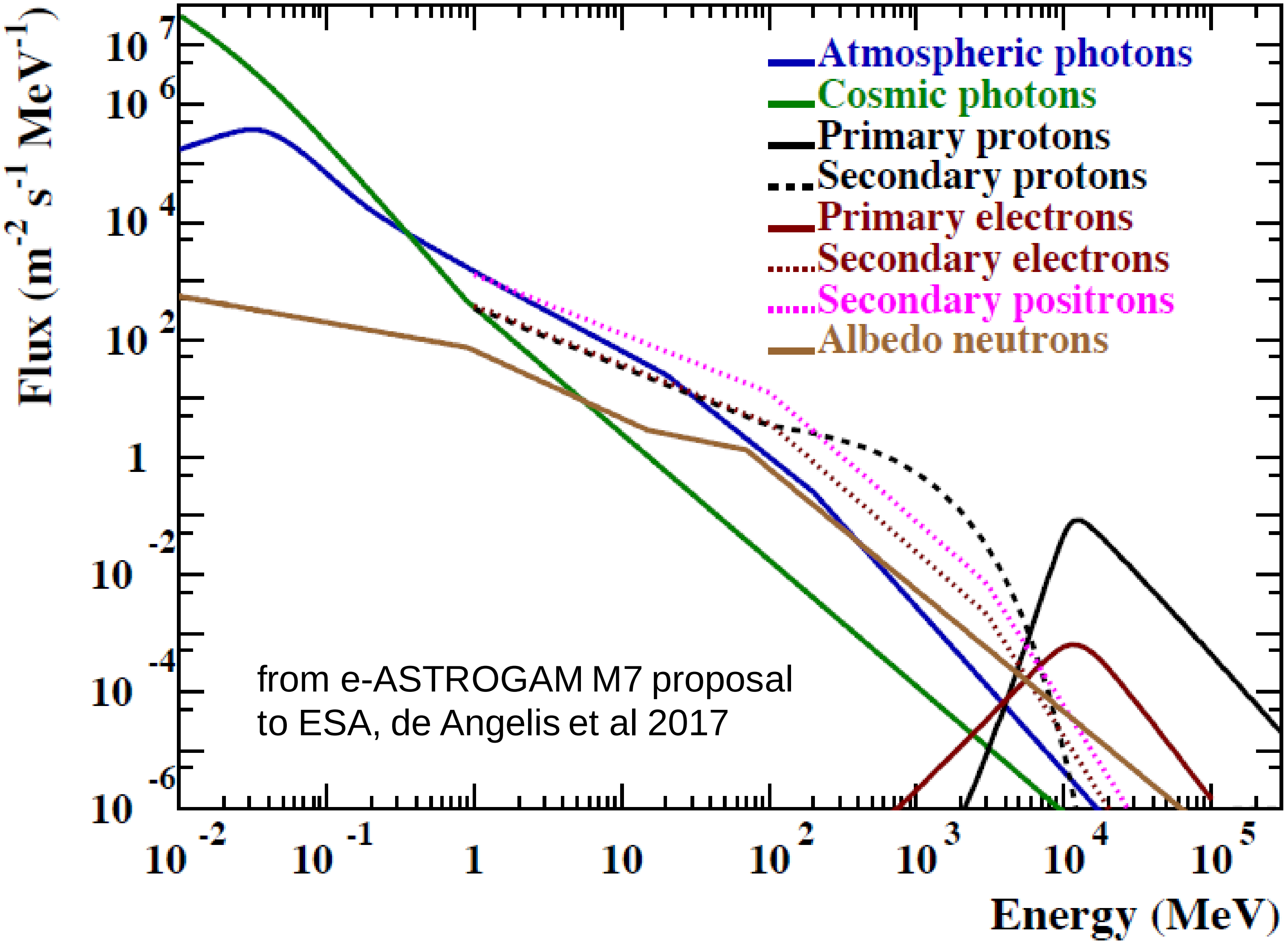

from e-ASTROGAM M7 proposal to ESA, de Angelis et al 2017

Earth shielding

- ✓ Irradiation is larger in high orbit (outside the Earth magnetic field) ➔ most gamma-ray instruments are in low orbits
- ✓ They also try to avoid the south-Atlantic anomaly and the poles ➔ equatorial orbit best

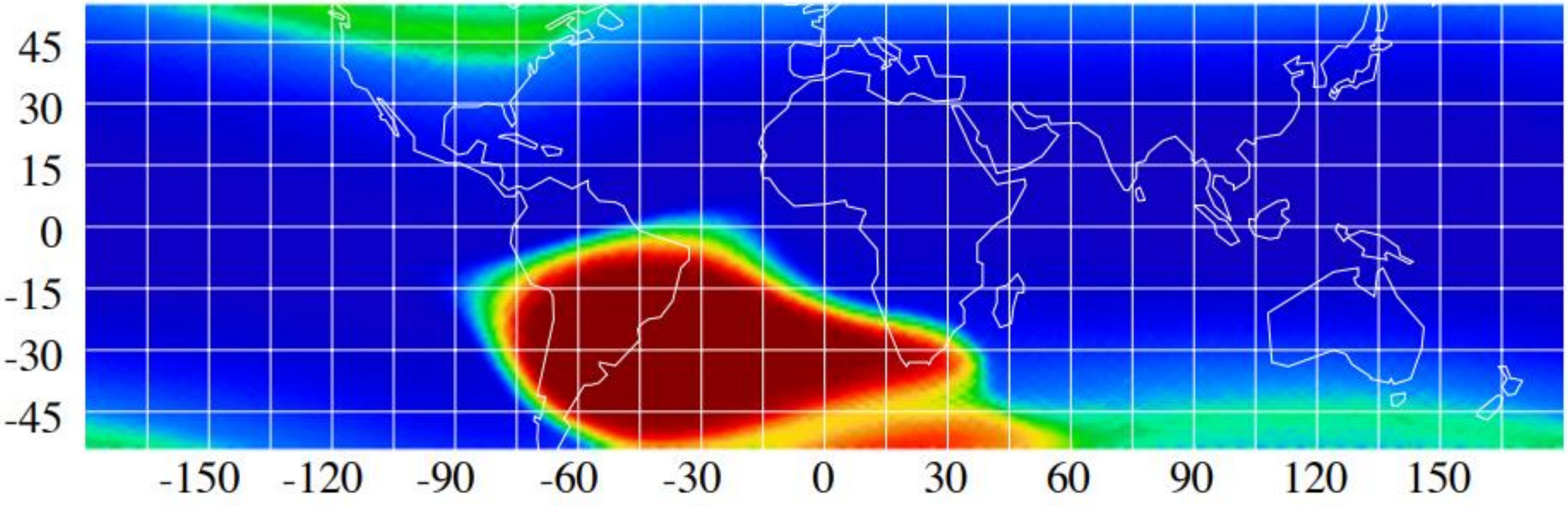

Particle environment seen by ROSAT in the 1990s (credit S. Snowden)

Particle background

- ✓ Reduce the background by an anti-coincidence (veto) device
- ✓ Detect charged particles, typically by a **plastic scintillator** that does not absorb the gamma rays
- ✓ Reject interactions in a small time window around the AC signal
- ✓ Segment the ACD to reduce self veto by backsplash (veto only events that come through this tile)
- ✓ Avoid dead areas between the tiles
- ✓ Very good efficiency (0.9997 in Fermi-LAT)

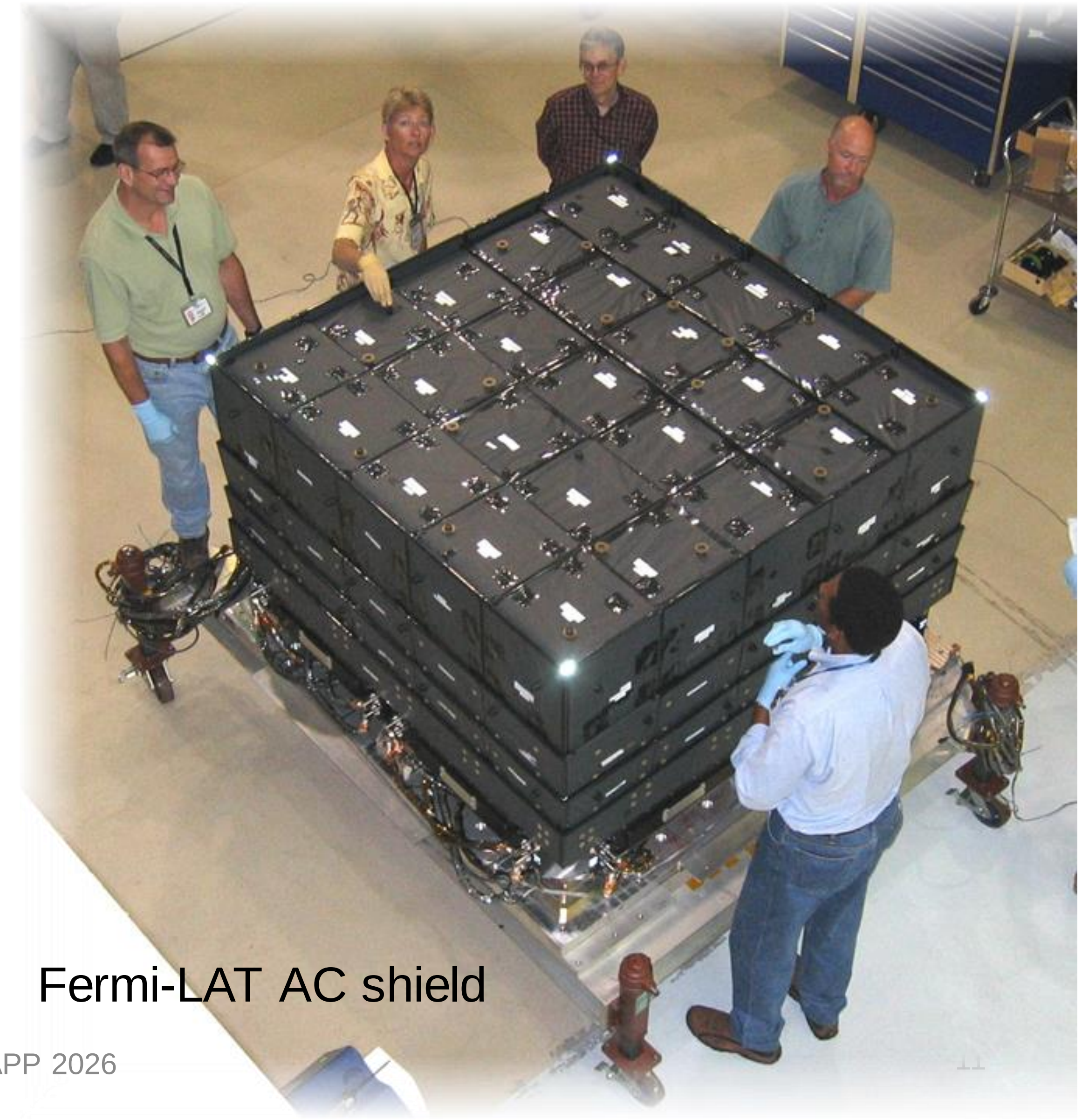

Fermi-LAT AC shield

Sky background

- ✓ In the GeV range the sky background (Galactic interstellar emission mostly) is larger than the residual charged-particle background
- ✓ Must be modelled accurately (to the % level) to detect point sources and small extended sources on top of it
- ✓ Mostly follows interstellar gas, but other components ➔ **major difficulty**

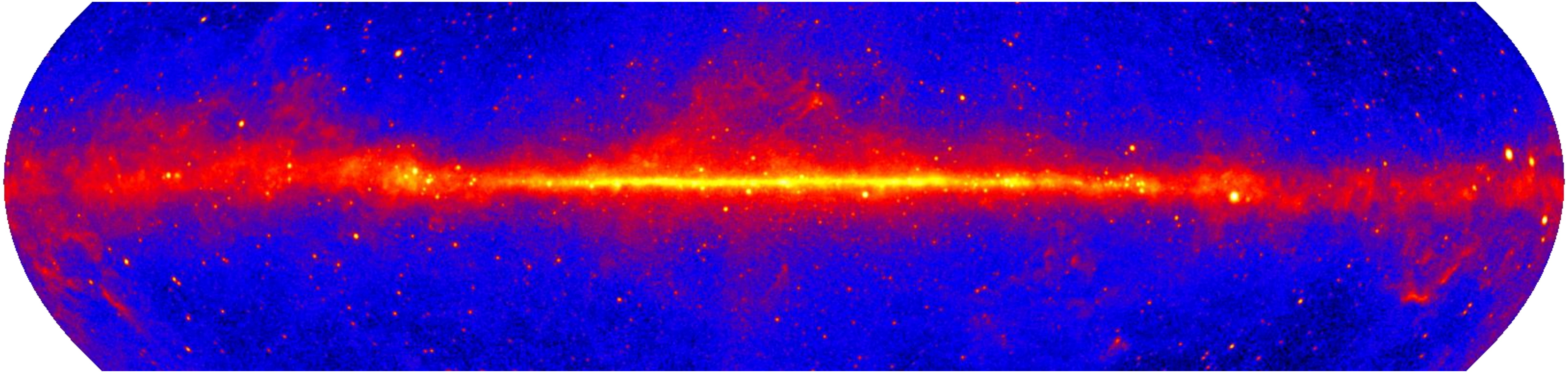

III. Photoelectric detectors

Localisation by geometry

Photoelectric detection is simple but cannot lead to an estimate of the photon direction (only the interaction point)

Mirrors (telescopes) cannot be used easily beyond 100 keV

Gamma-ray burst detectors (BATSE, Fermi GBM) work in the sub MeV range and use heavy scintillators to favor photoelectric effect

Localisation is done statistically by comparing fluxes from several detectors oriented in different ways

This is very rough (several degrees)

Four groups of three NaI detectors to cover the full sky

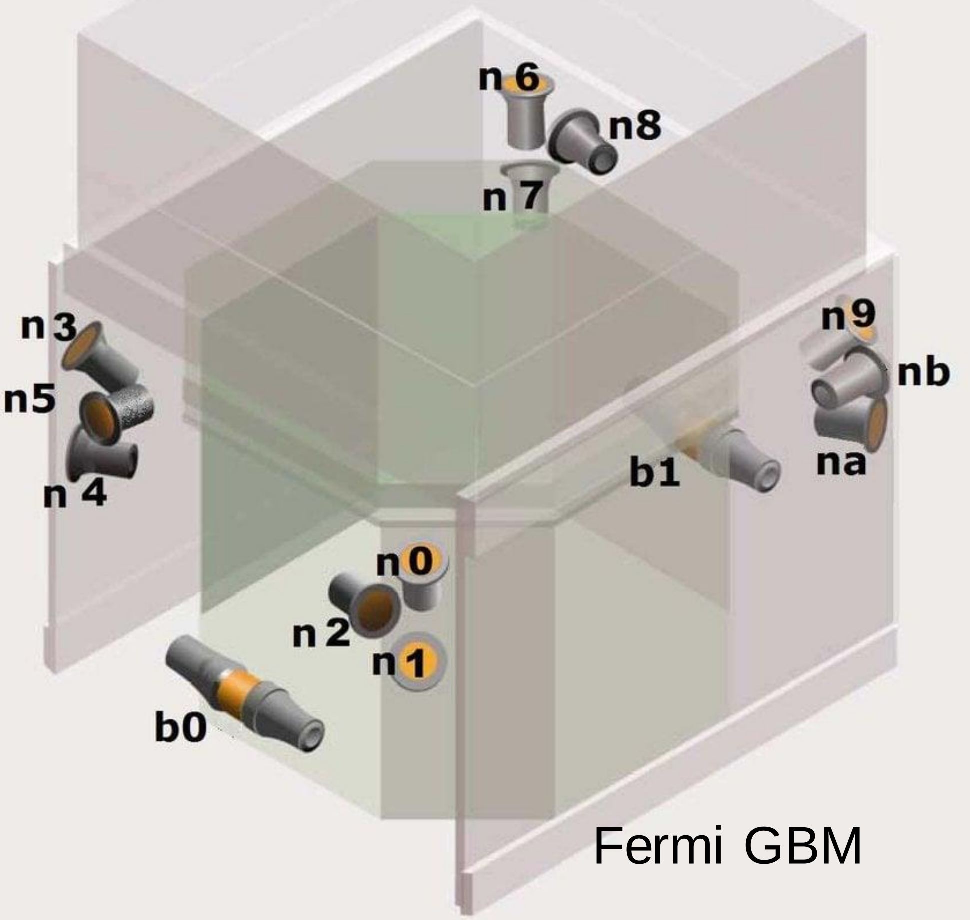

Fermi GBM

Localisation by timing

A completely different localisation method is from timing, when **the source varies** at the second time scale (GRB)

Aligning the arrival times of GRB events on two detectors far apart provides a **ring** on the sky

Three detectors give two directions, four or more just one direction

The **angular resolution** is related to the GRB time scale δt and the distance D

$$\sin\theta \;\, d\theta = {}^{c\,\delta t}/_{D}$$

It becomes **quite good** (0.1°) for δt = 1 s and D = 1 a.u. (1.5 10^8 km)

IPN (InterPlanetary Network)

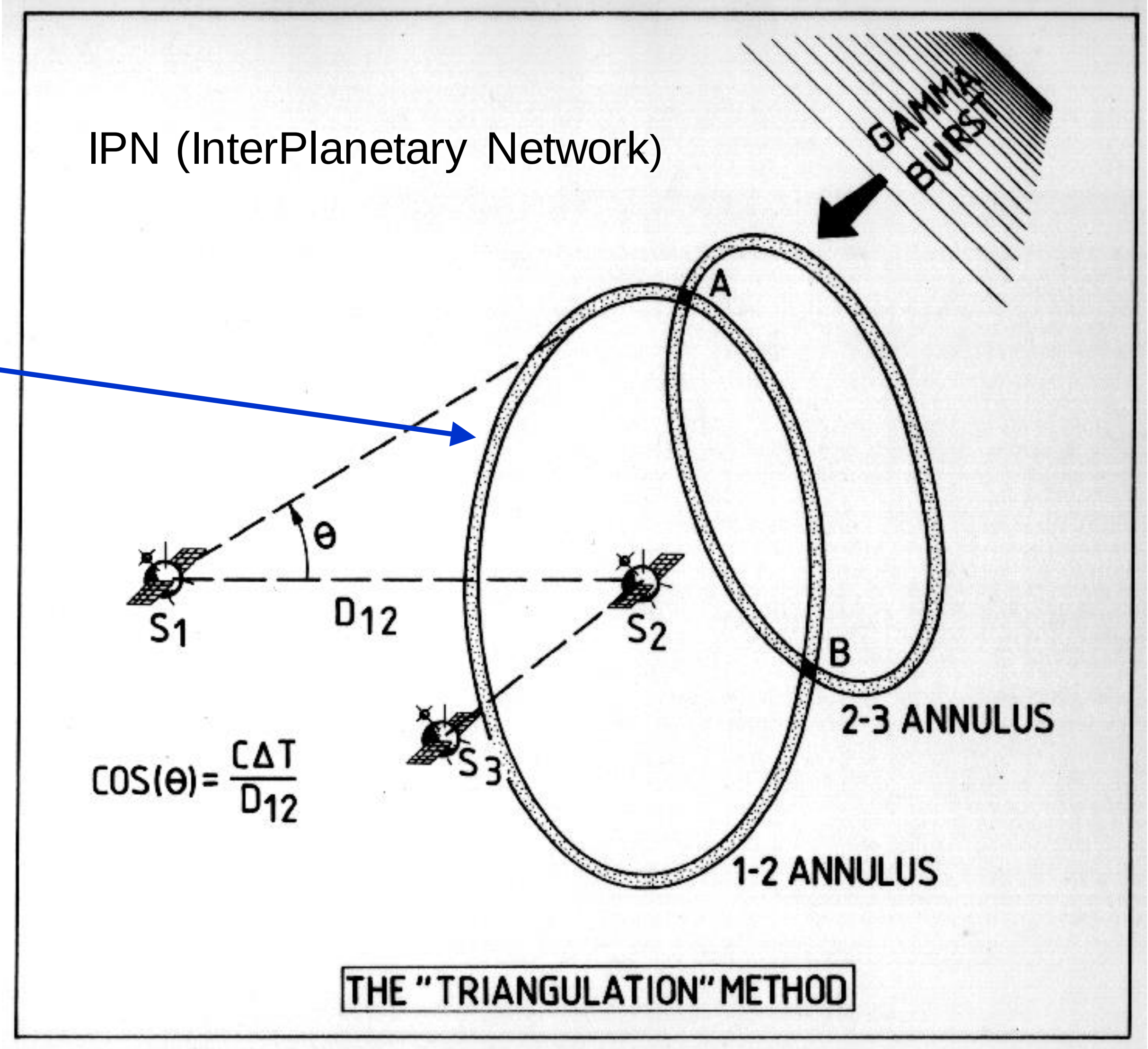

Localisation by coded mask

Sources that are not time variable can be localized by **obscuration**

One cm or so of W elements can block incoming photons, letting them in only through empty elements

The imaging detector records the **image of the mask** offset by $H \tan\theta$

The **angular resolution** is related to the mask element size *a* and the distance to the detector *H*

$$d\theta / \cos^2\theta = a / H$$

It is **quite good** (0.2°) for a = 1 cm and H = 3 m

Applied in INTEGRAL, Swift/BAT, ASTROSAT, SVOM/ECLAIRs

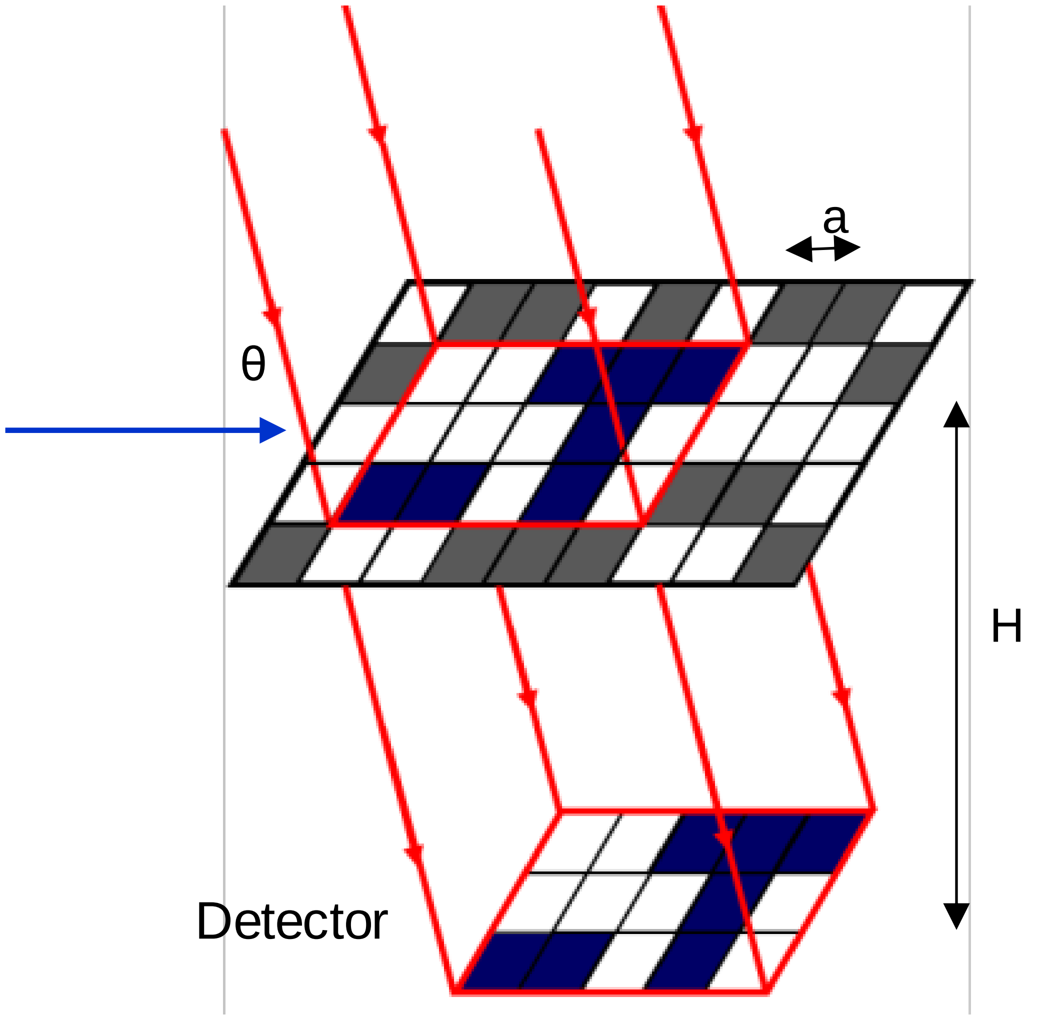

Geometry for coded mask

The mask must be bigger than the detector (eg $l_M = 2\ l_D$)

The distance between the mask and the detector is shielded from the sky to avoid non-coded background

The fully coded field of view (**FCFOV**) is the set of sky positions that project a full mask pattern

Sources outside the FCFOV project only a fraction of the mask: they are **partially coded**

For l_D = 50 cm, l_M = 1 m and H = 3 m, the **FCFOV** is defined by $\tan\varphi = (l_M - l_D) / (2\ H)$ ➔ φ = 4.75° so the **FCFOV** is a square 9.5 x 9.5° in the sky

The extreme limit of the **PCFOV** (ZRFOV) is defined by $\tan\psi = (l_M + l_D) / (2\ H)$ ➔ ψ = 14° so the **PCFOV** is a square 28 x 28° in the sky

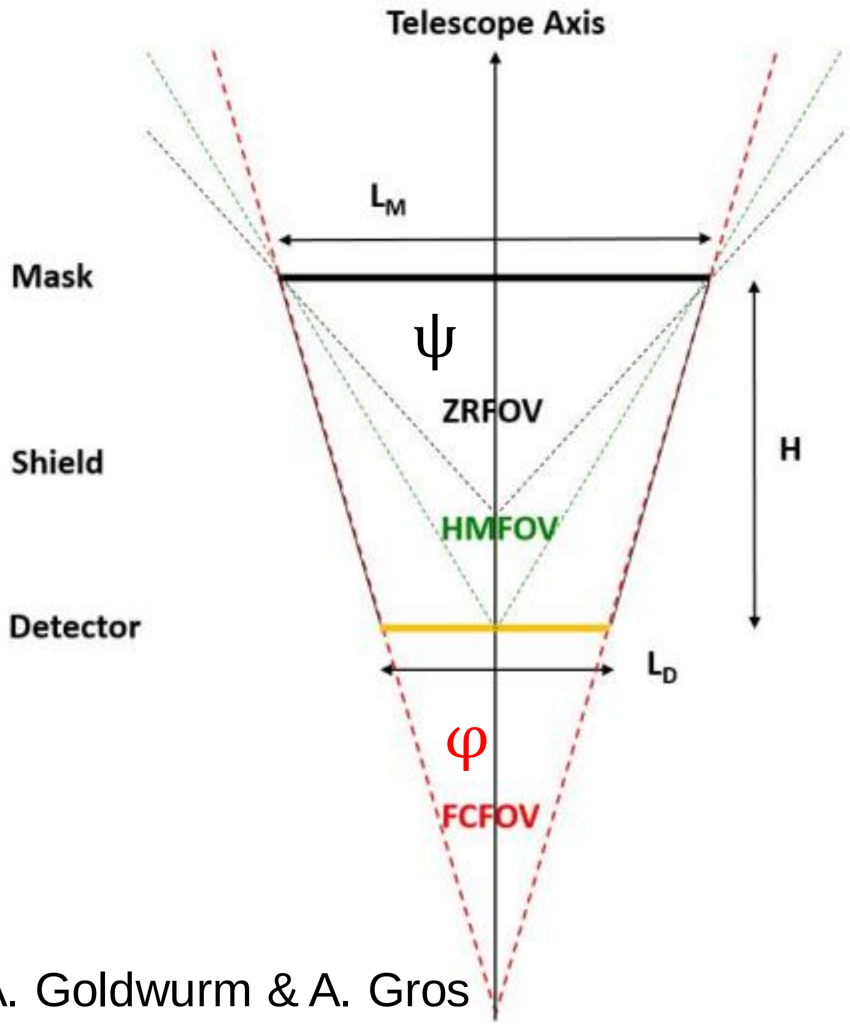

A. Goldwurm & A. Gros 2023, arXiv 2305.10130

Reconstruction by coded mask

The mask must be designed so that no two different directions project the same pattern

Each pixel inside the PCFOV can be tested by correlating the part of the detector that it would illuminate with the part of the mask that it would go through

The mask can be designed so that the correlation will give 0 for other pixels inside the FCFOV, but not outside

The highest peak corresponds to the source direction

Secondary peaks can be eliminated after the source flux is estimated from the highest peak

The **background** for all sources is **all counts** recorded on the detector ➔ **not very sensitive**

Image

Mask

Reconstructed sky

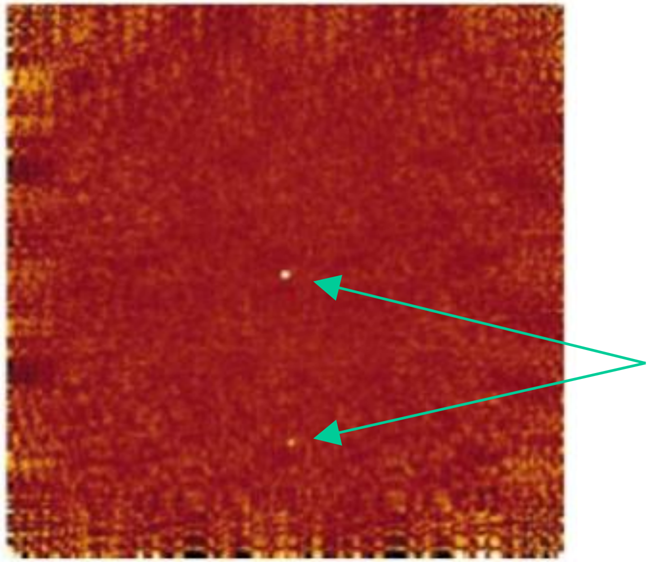

INTEGRAL, Goldwurm & Gros 2023

IV. Compton detectors

Compton effect

In the **Compton effect** the incoming photon of energy E_0 cedes a fraction of its energy E_1 to an **electron** of the material (binding energy assumed small).

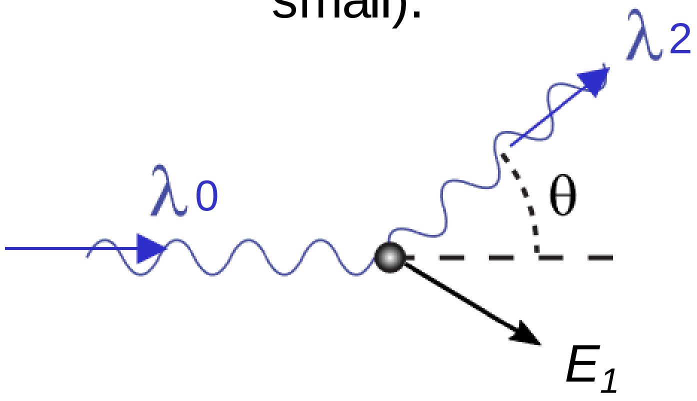

$$\lambda_2 = \lambda_0 + \lambda_c(1 - \cos\theta)$$

$$\lambda_c = {}^{h}/_{m_e c} = 2.43\ 10^{-12}\ \text{m} \leftrightarrow\ 511\ \text{keV}$$

$$1 - \cos\theta = m_e c^2 \left({}^{1}/_{E_2} - {}^{1}/_{E_0} \right) = {}^{1}/_{\gamma_2} - {}^{1}/_{\gamma_0}$$

$\gamma = {}^{E}/_{m_e c^2}$ expresses photon energies in units of the **electron mass**

A front scatter changes nearly nothing while a back scatter results in maximal reduction of the photon energy.

Compton scattering angle distribution

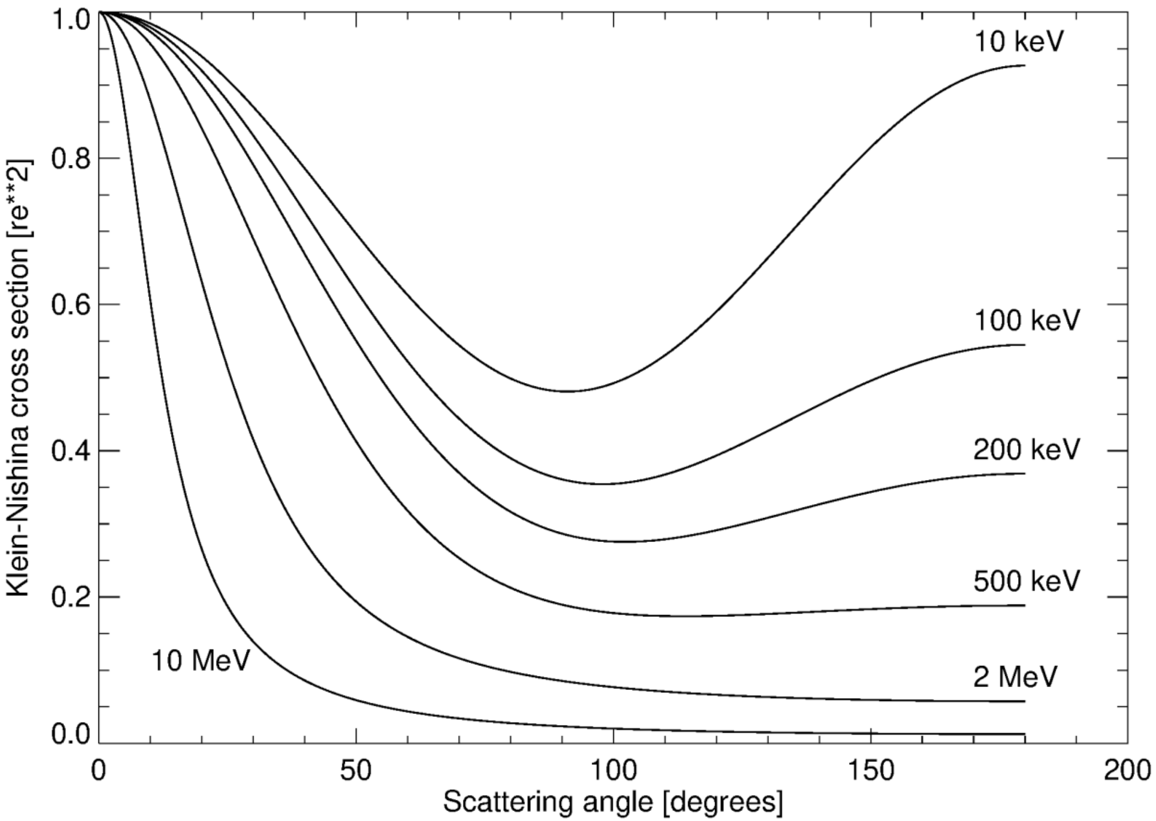

The probability of scattering as a function of θ is given by the **Klein-Nishina** cross section

$$\frac{d\sigma}{d\Omega} = \frac{r_e^2}{2}\left(\frac{E_2}{E_0}\right)^2 \left(\frac{E_2}{E_0} + \frac{E_0}{E_2} - \sin^2\theta\right)$$

which can be written as a function of θ parametrized by E_0 using

$$\frac{E_0}{E_2} = \frac{\gamma_0}{\gamma_2} = 1 + \gamma_0(1 - \cos\theta)$$

little back scattering above 511 keV, mostly forward

Compton detection

Photon detection and characterization via the **Compton effect** requires

1. Measuring precisely the **position** of the first interaction
2. Measuring precisely the **position** of the second interaction

→ **3D detection of electrons** (e.g. Si strips)

3. Knowing the order of interactions → analyse the full chain
4. Measuring precisely the first electron **energy** E_1
5. Measuring the **energy** left in all subsequent interactions

→ e.g. Si to convert into **electron-hole pairs**

1 and 2 give the reference **direction**

4 and 5 give the incoming **energy** $E_0 = E_2 + E_1$ (if only 2 interactions)

3, 4 and 5 give the scattering **angle** θ via the Compton equation

Compton geometry

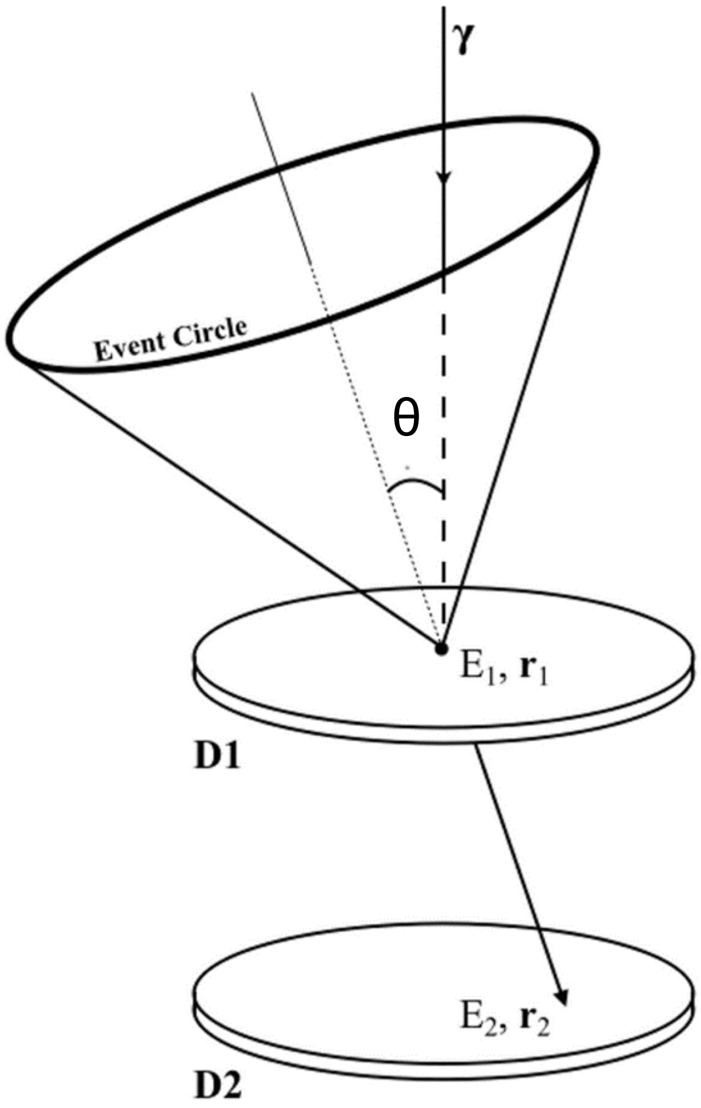

The **line** between the two interaction points $\mathbf{r_1}$ and $\mathbf{r_2}$ defines an **axis** in the detector geometry.

cosθ obtained from E_1 and E_2 via the Compton formula then defines a **ring** on the sphere

$$\cos\theta = 1 - \frac{E_1\, m_e c^2}{E_2(E_1 + E_2)}$$

The width of the ring sinθ dθ is the **angular resolution** and depends on the **precision in measuring the energies** dE_1 and dE_2
The **positions** $\mathbf{r_1}$ and $\mathbf{r_2}$ can in general be measured accurately

Above several MeV the photon may experience **several Compton interactions** in the detector. Their **order** must be inferred by checking **consistencies** between energies and angles

COMPTEL, Schönfelder & Kanbach 2013; Excellent reference there

Compton: energy and angular resolution

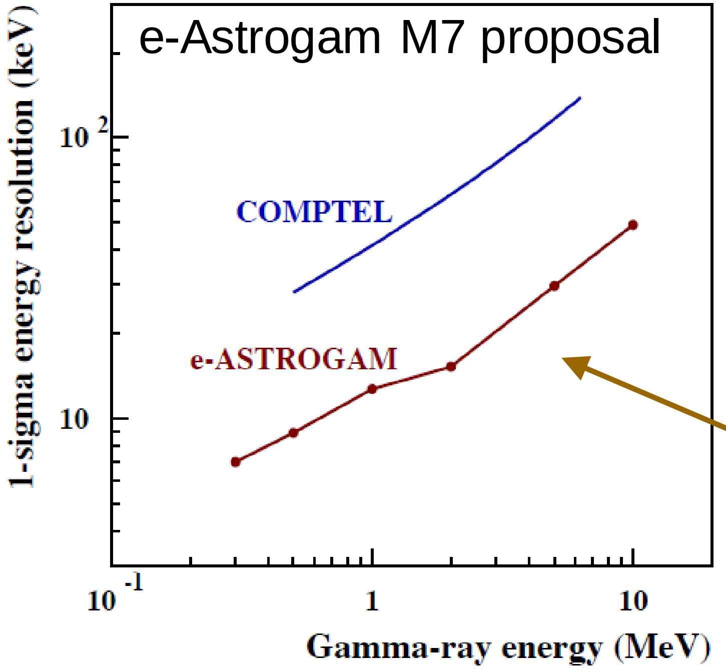

Modern Si detectors can improve significantly on COMPTEL in terms of **energy resolution** (Ge detectors are even better, see later)

They can reach an **energy resolution** *E/ΔE* of about 100 at 1 MeV, improving with energy

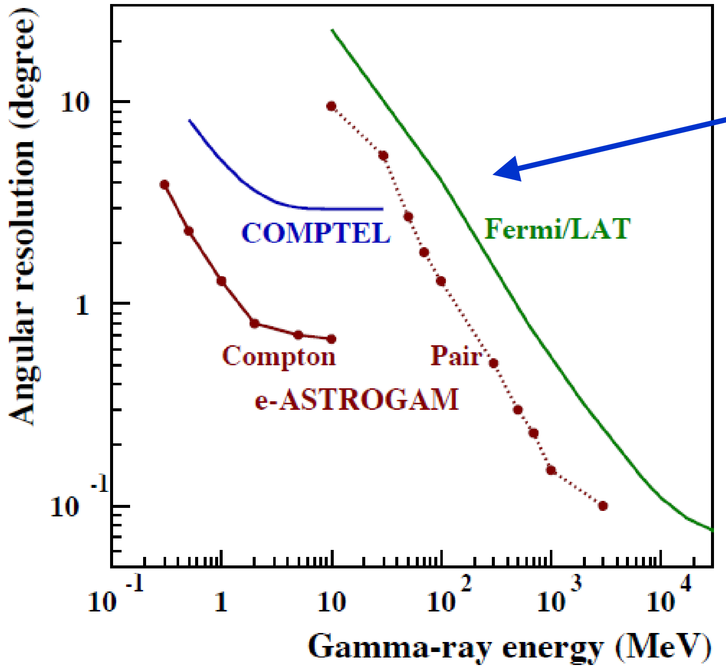

The resulting **angular resolution** can be better than 1° FWHM above 1 MeV, worsening to 3° at 300 keV

This is comparable to pair-creation detectors

Compton: source detection

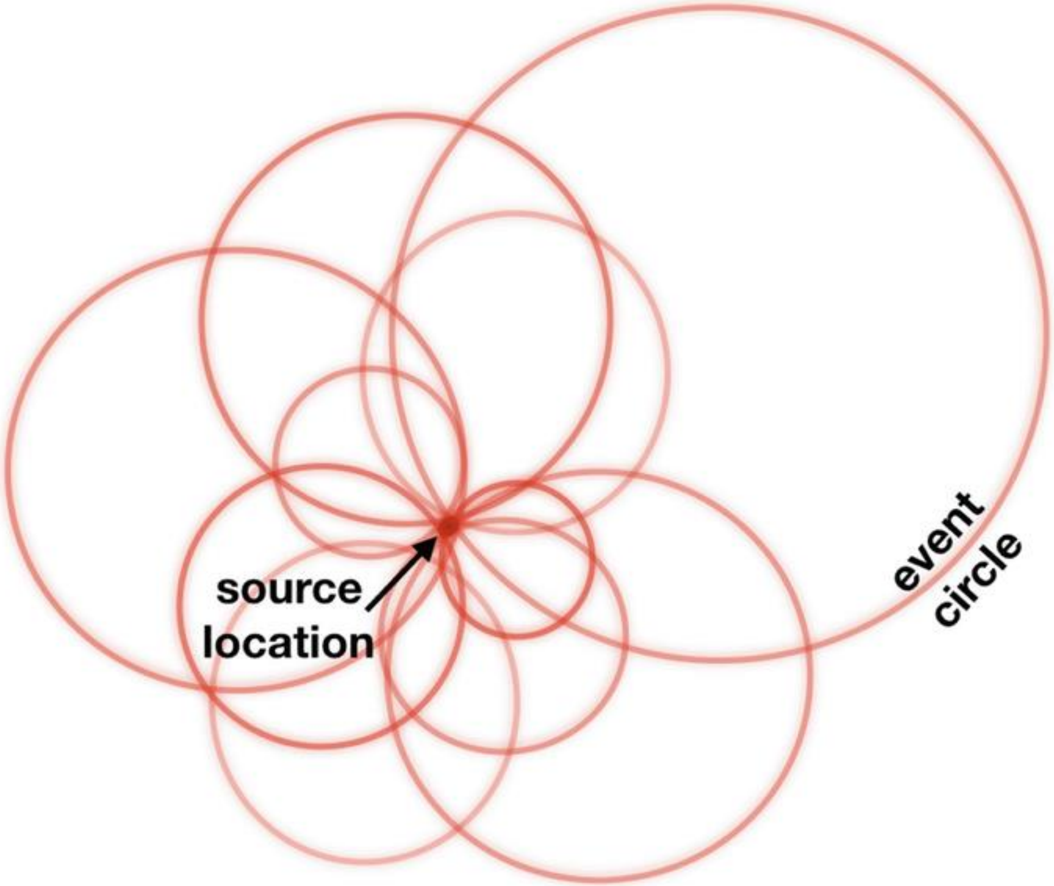

An **individual photon** does not point directly at the source (only a ring)

But a **collection of photons** (all with different event circles) can

Sources are all observed at the same time, so it is not known a priori which circle corresponds to which source

But this can be done **statistically**

If the electron can be **tracked**, the azimuthal angle can be constrained and the circle reduced to an **arc**

Compton detector

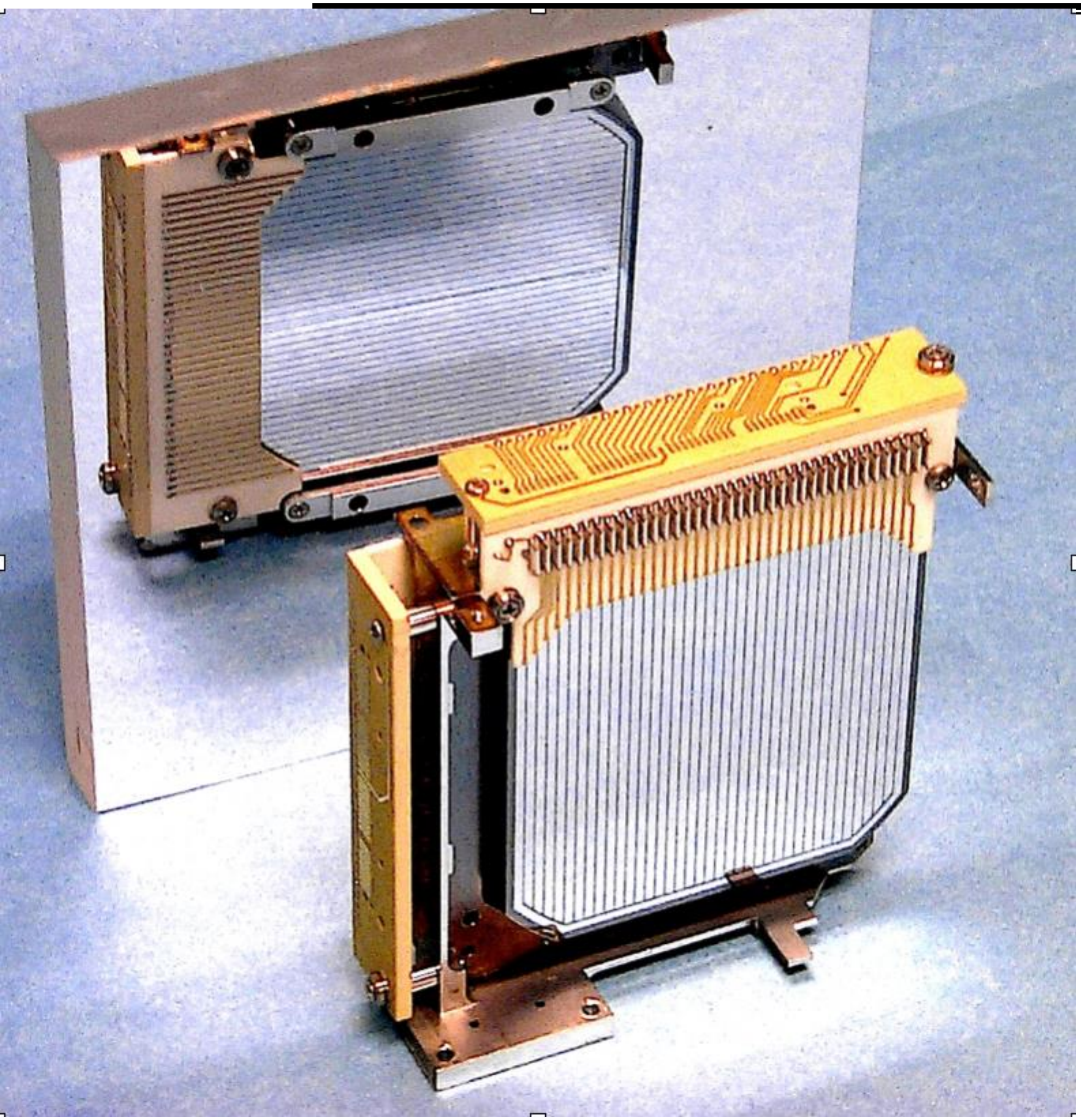

COSI (NASA SMEX, launch 2029)

Full instrumented volume

The detector is most often **layers of Si** (cheap, easy to work with, can build large detectors)

Drawback of Si is that the energy resolution (hence the PSF as well) is not excellent

In COSI the detector is **layers of Ge** (more difficult to operate, must be cooled at -200° C) that has excellent spectral resolution

Strips in both directions to measure the interaction point

Compton: sensitivity

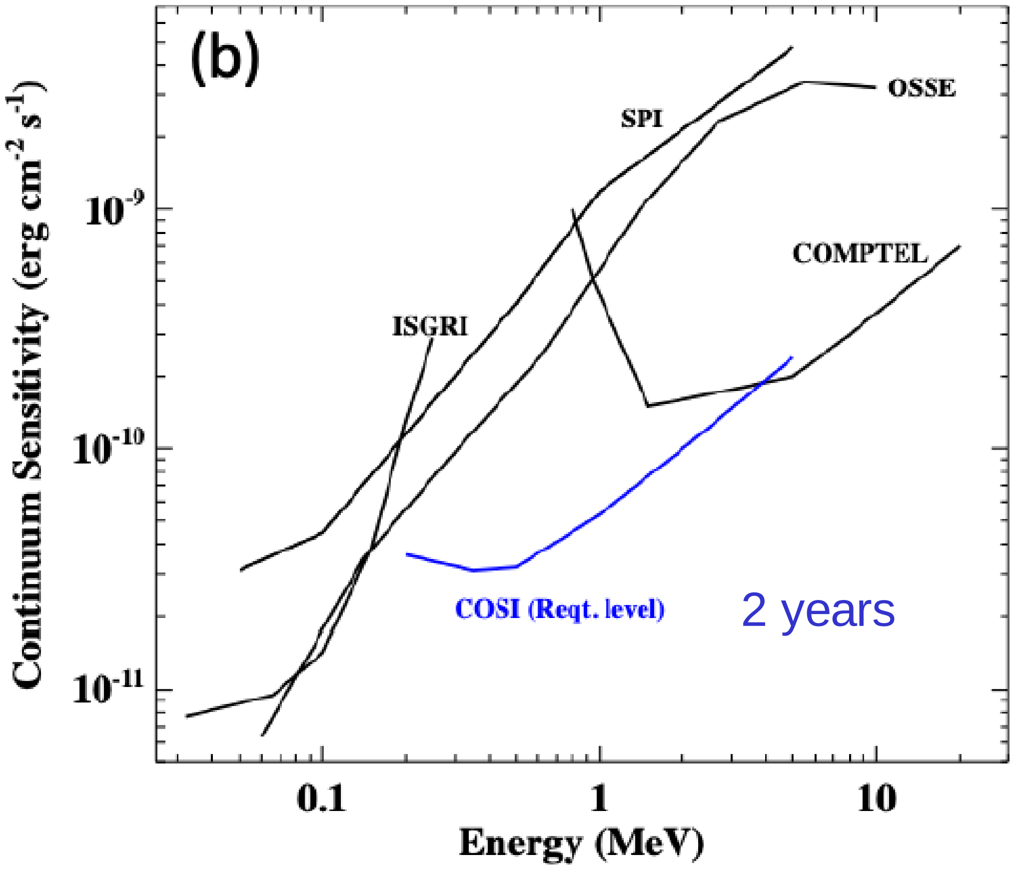

COSI (NASA SMEX, launch 2029)

COSI is a small instrument (400 kg, 50 cm)

But it can do better than COMPTEL and INTEGRAL between 200 keV and 2 MeV

The sensitivity of current Compton instruments remains however **far above** Fermi-LAT in the adjacent GeV domain (10^{-12} erg/cm2/s)

This energy range remains **poorly covered**

Compton detector limit

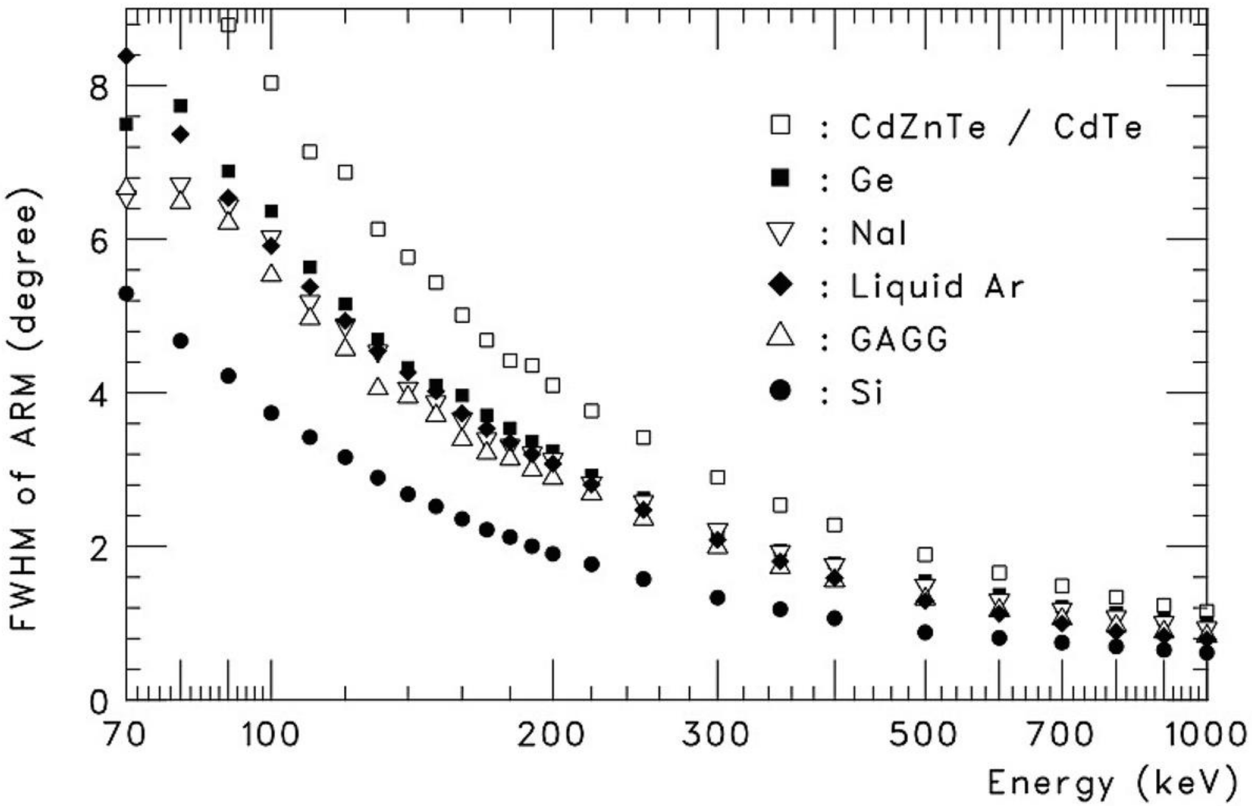

The energy and angular resolution hit a **fundamental limit** due to the **binding energy** of electrons that introduces an irreducible uncertainty (« Doppler broadening »)

That uncertainty increases with Z, so it is larger in Ge than in Si

Compton: polarisation

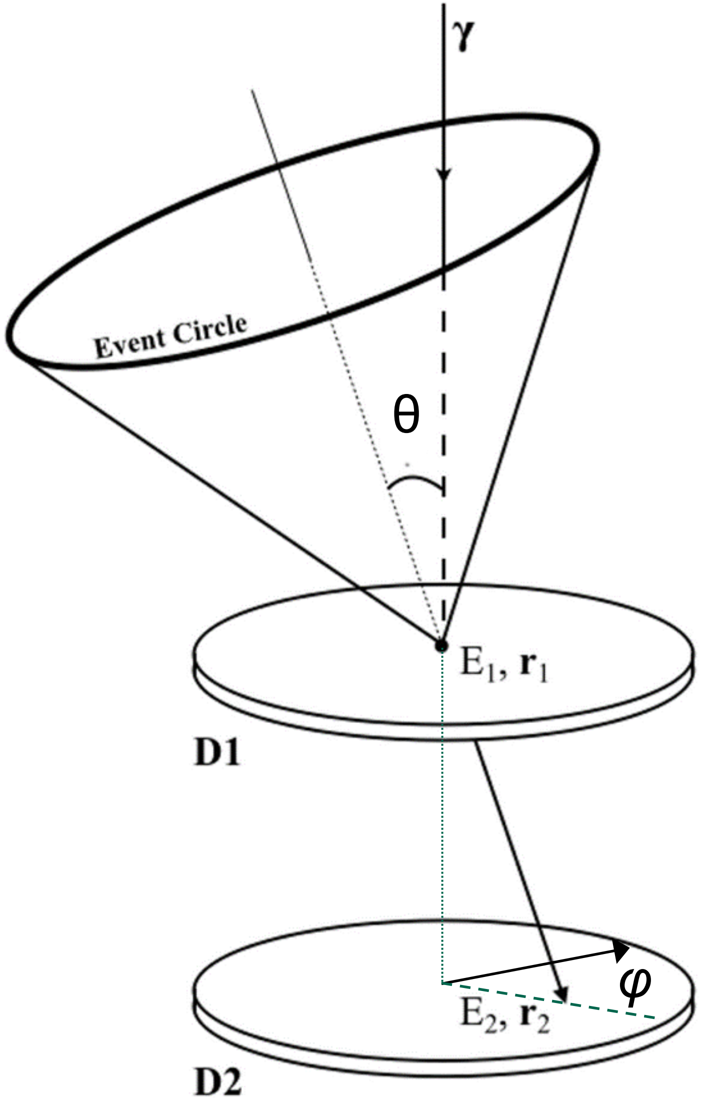

The **Compton effect** is sensitive to the **linear polarisation** of the incoming photons.

The Klein-Nishina cross section at the first interaction depends on the azimuthal angle φ of the ejected electron (or the scattered photon, since they are in the same plane) with respect to the polarisation direction φ_0 as

$$\frac{d\sigma}{d\Omega} = \frac{r_e^2}{2}\left(\frac{E_2}{E_0}\right)^2\left(\frac{E_2}{E_0} + \frac{E_0}{E_2} - 2\sin^2\theta\cos^2(\varphi - \varphi_0)\right)$$

Compton: polarisation

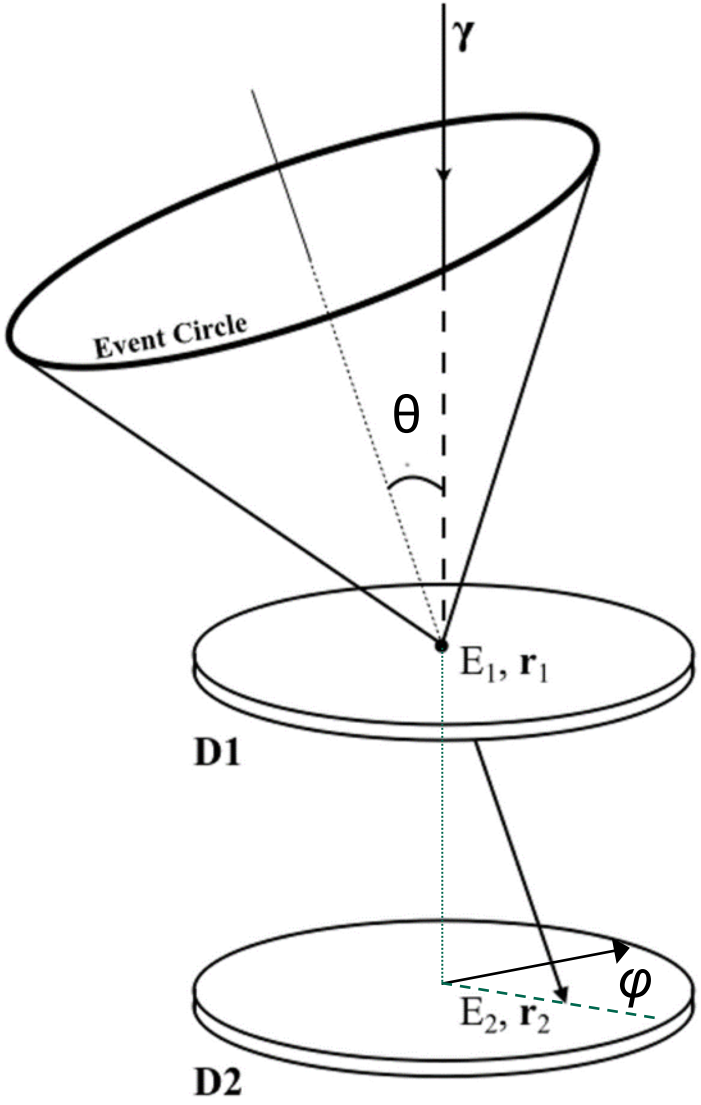

$$\frac{d\sigma}{d\Omega} = \frac{r_e^2}{2}\left(\frac{E_2}{E_0}\right)^2\left(\frac{E_2}{E_0} + \frac{E_0}{E_2} - 2\sin^2\theta\cos^2(\varphi - \varphi_0)\right)$$

E_2/E_1 and θ change for each photon coming from the source, but this results in a net **flux modulation as a function of φ**

$$S = \bar{S}\left[1 + a\cos\left(2(\varphi - \varphi_0)\right)\right]$$

where φ_0 is the polarisation angle of the source. a is typically < 20%.

Conversely, **measuring the angle φ** (if the electron is traced, or the source direction is known) can tell whether the source is polarised.

V. Pair-production detectors

Pair-production process

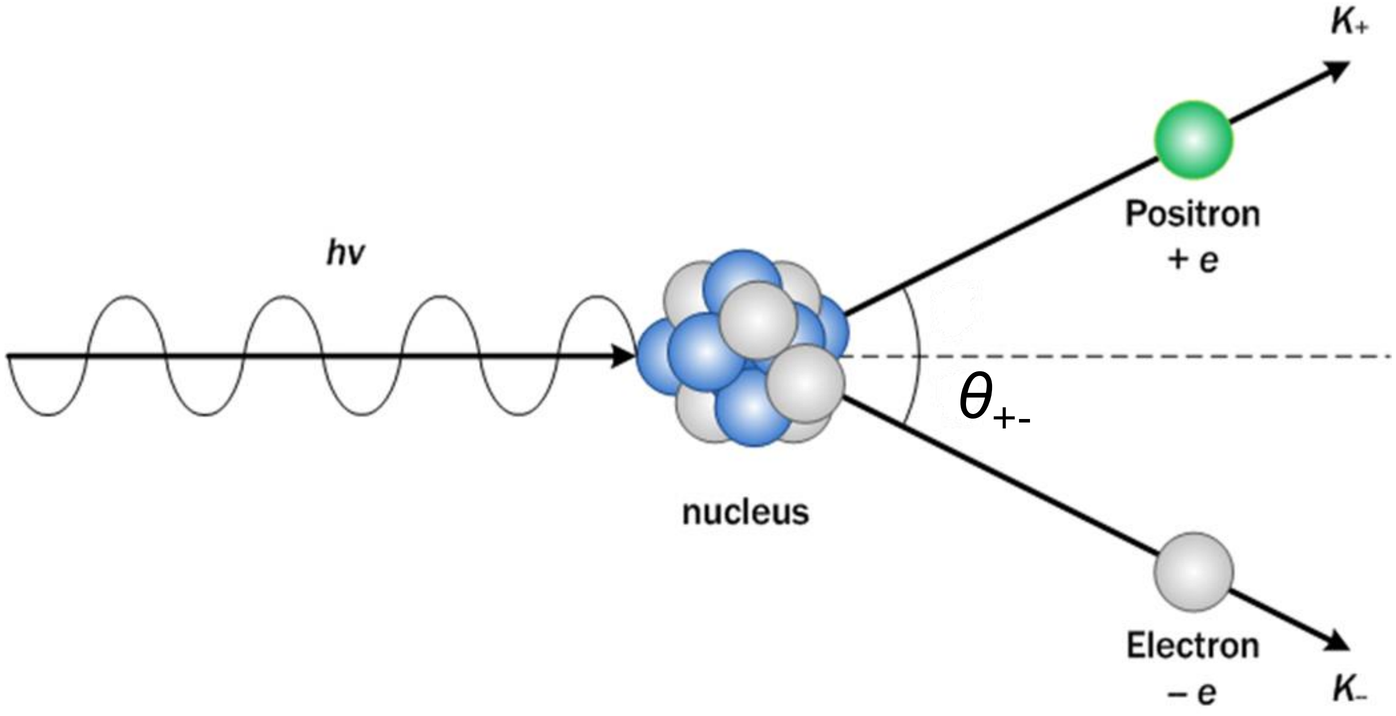

$h\nu + A \rightarrow e^+ + e^- + A$

Momentum is partly absorbed by the nucleus A, but **energy** is transmitted nearly whole to the pair:

$$E_+ + E_- \approx h\nu - 2\, m_e\, c^2$$

Energy threshold

$2\, m_e\, c^2\, (1 + m_e/m_A) \approx 1.022$ MeV

Process becomes dominant above 10 MeV or so

Pair-production process

Pair-production happens preferentially in **heavy materials** (mass attenuation in $cm^2/g \propto Z$)

Opening angle θ_{+-} decreases as $1/E_0$
It is only 0.3° at 1 GeV

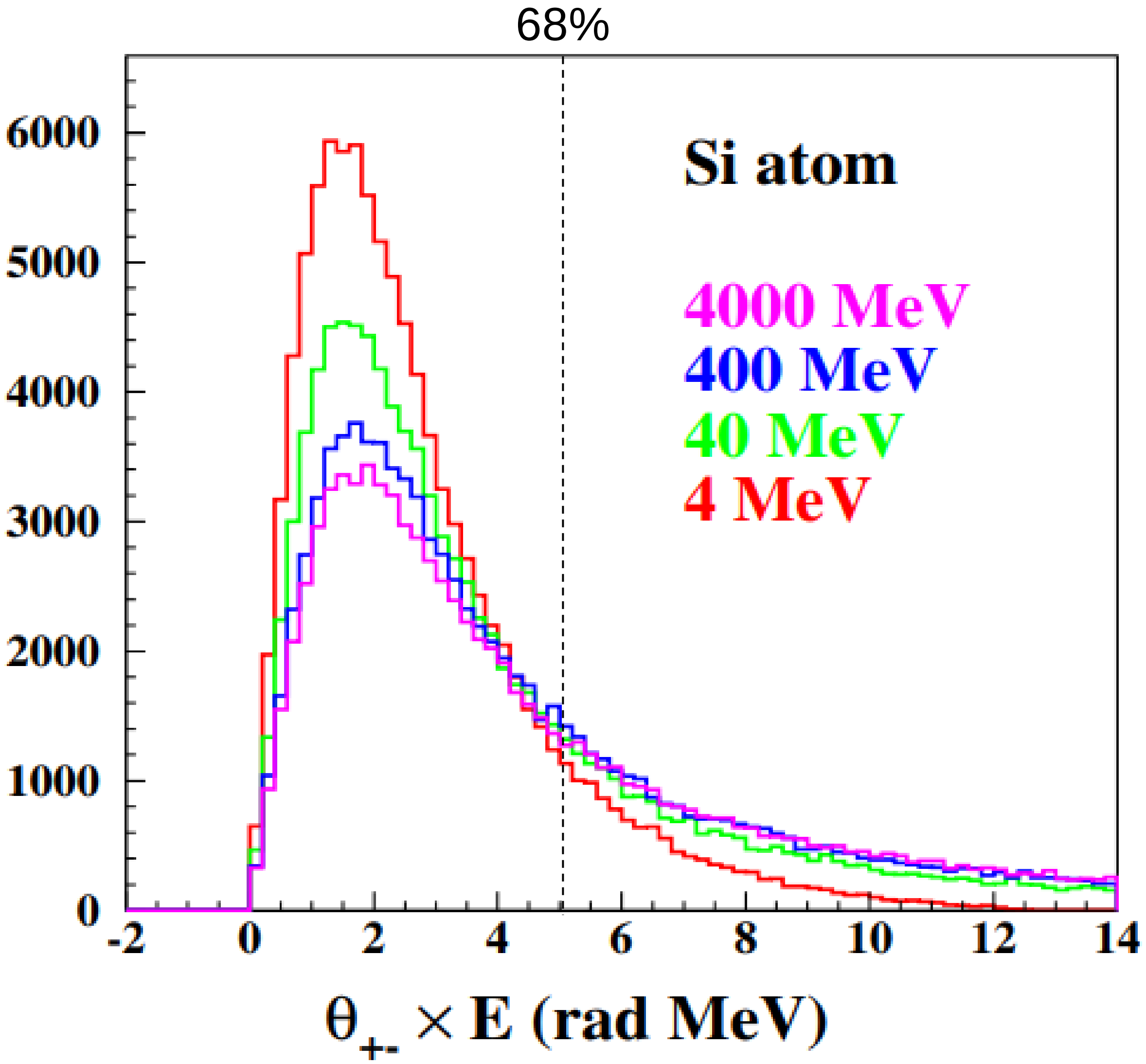

D. Bernard 2023, arXiv 2305.19690

Pair-production: electron fate

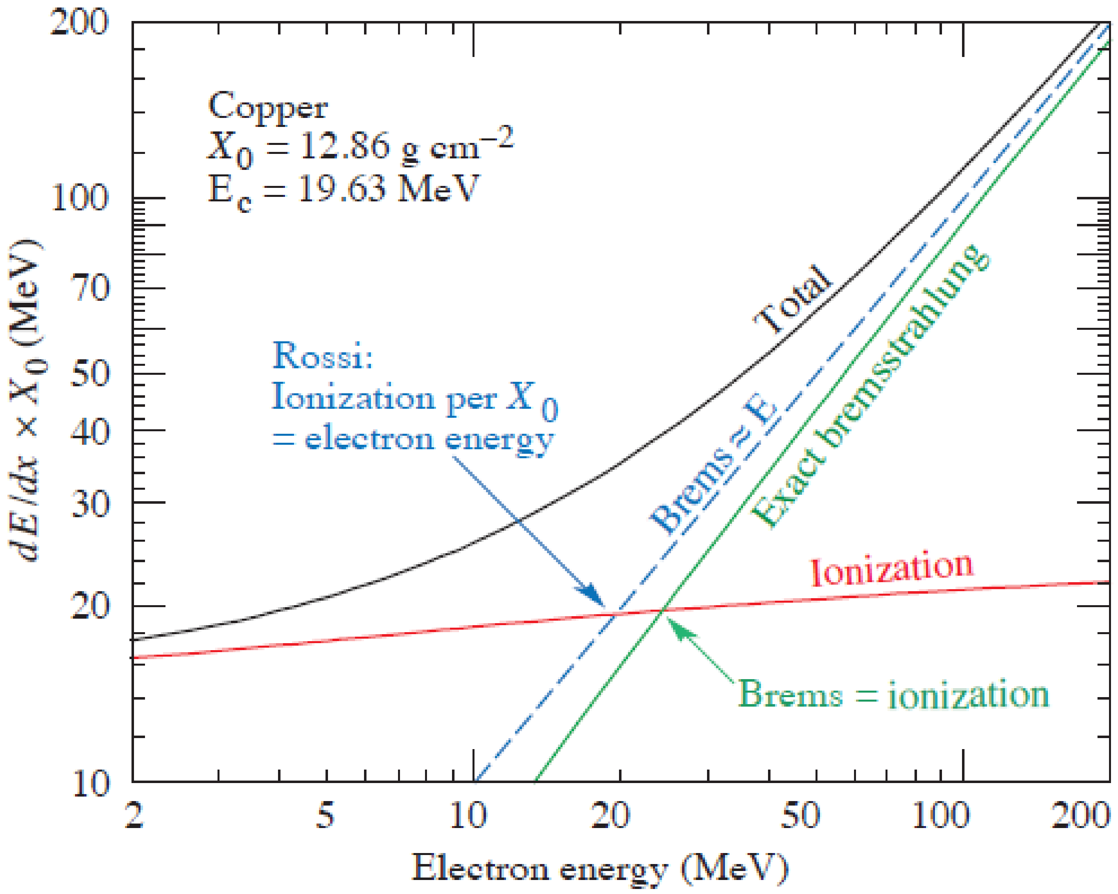

Particle Data Group 2020, chap 34

After the pair is created, the electron and positron interact with the material

Radiation length X_0: mean length over which the electron energy is divided by e by **bremsstrahlung**

It depends on the material but not much on the electron energy

Below critical energy E_c ≈ 10 MeV, fast loss to **ionization**

Pair-production: electromagnetic shower

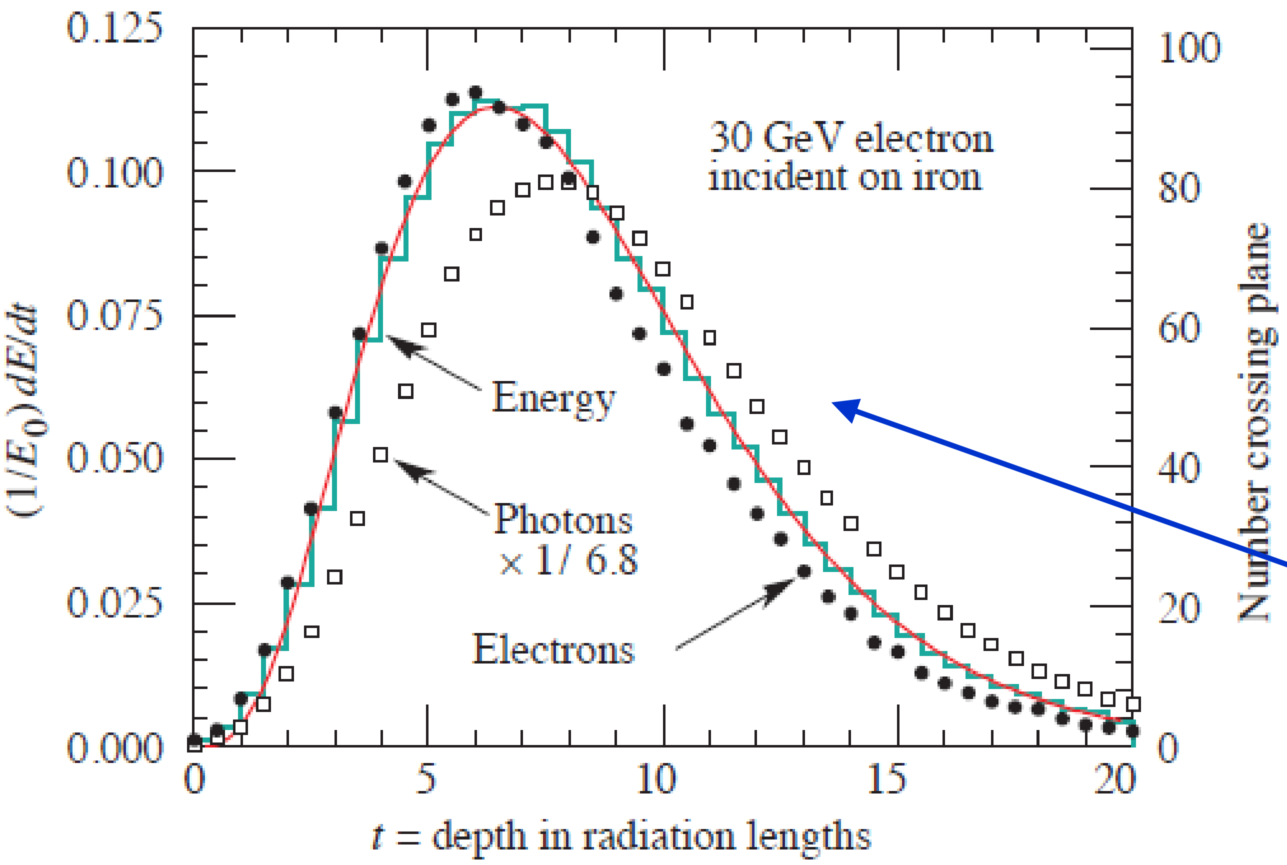

Particle Data Group 2020, chap 34

The bremsstrahlung photons occur at energies close to that of electron

They can create pairs again ➔ **shower**

red line / green histogram: **energy deposit** in the material (ends up as light that can be measured)

Hollow squares: current number of secondary photons

Filled circles: current number of electrons/positrons

Shower **peak** ≈ $\ln(E_0/E_c)$

Pair conversion principle

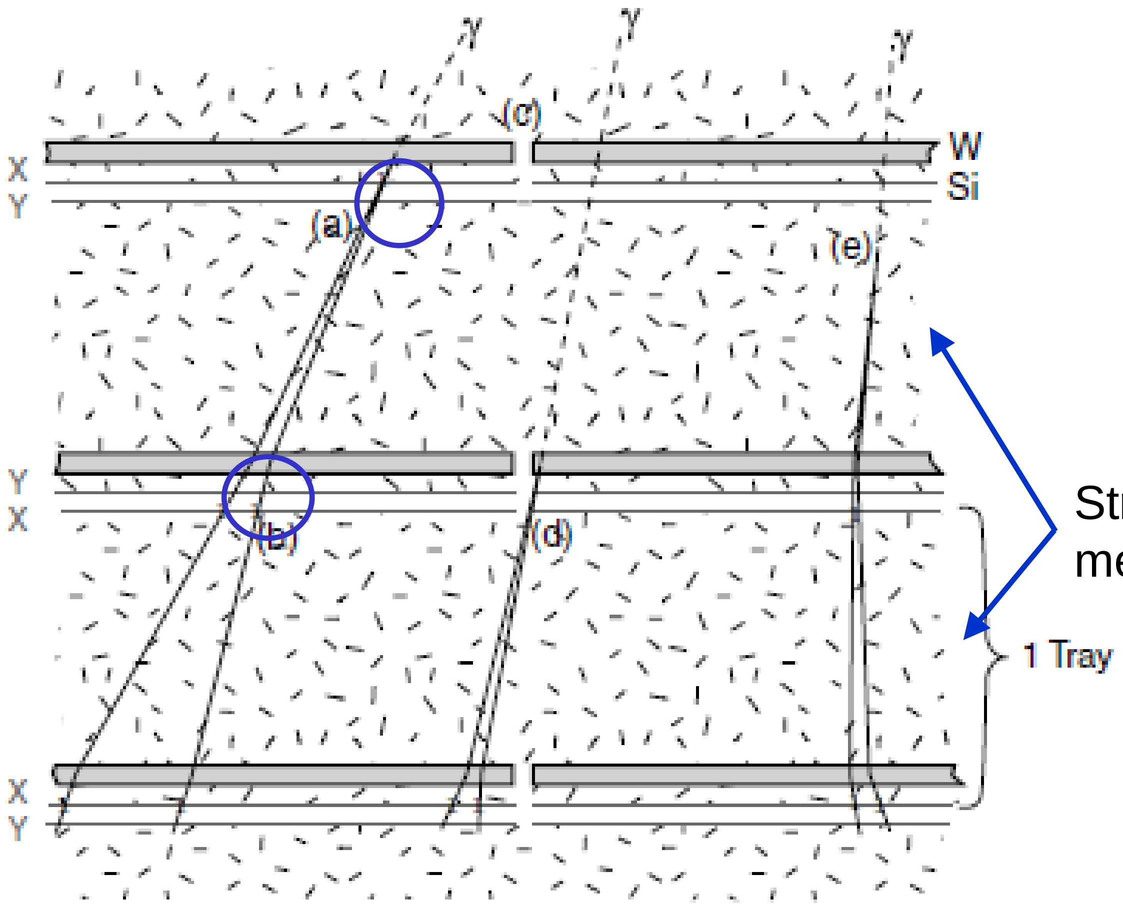

Tungsten **converters** where γ-rays can generate e+e- pairs
Follow electron **tracks** in light material sensitive to charged particles such as Si

The γ-ray **direction** is recovered from the tracks
Works above 10 MeV

Structure material in-between is carbon meant to minimize conversions in it

Each photon can be reconstructed **individually**, in direction as well as energy and time ➔ closer to **classical telescope** than MeV regime, and similar in spirit to TeV regime

Atwood *et al.* 2007, Astropart.Phys.28:422-434

Fermi Large Area Telescope

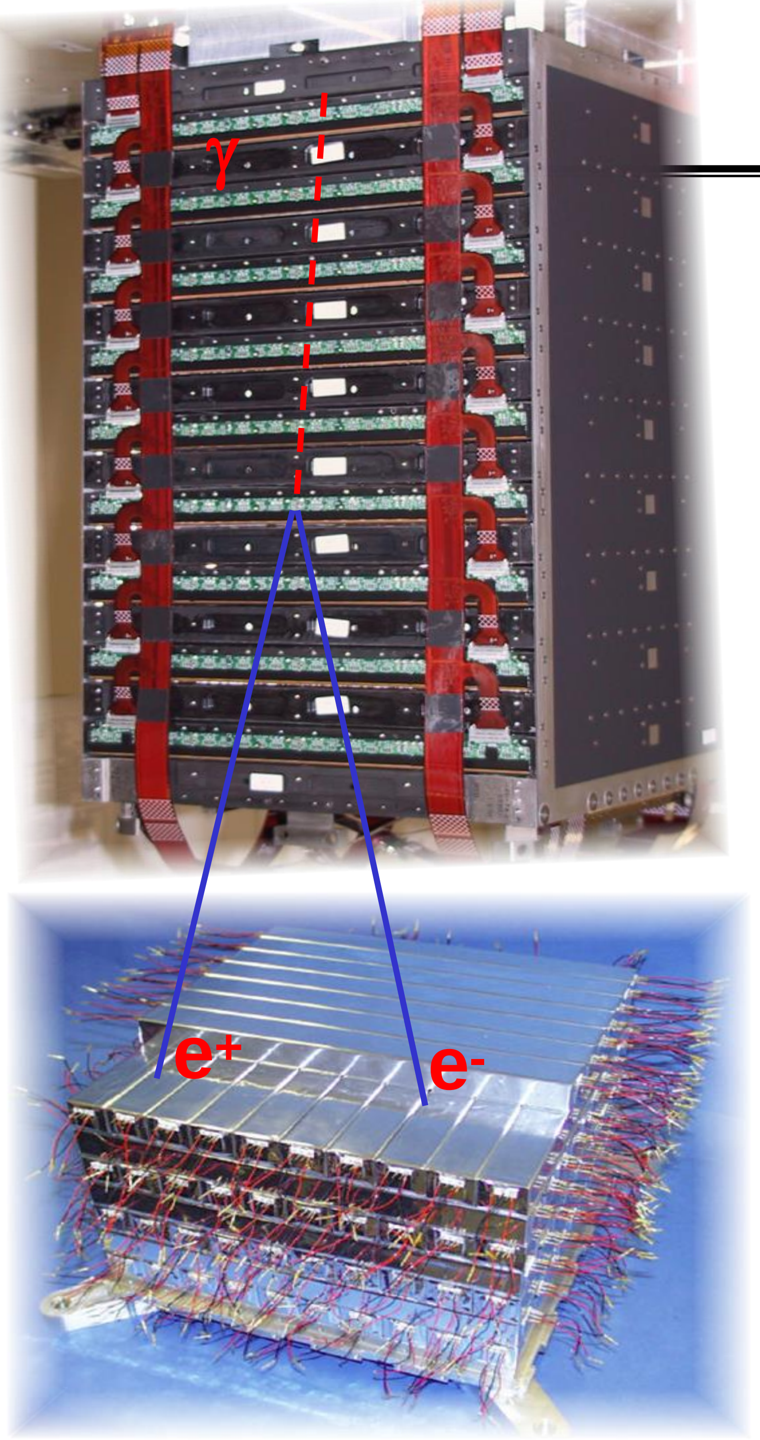

Tracker/Converter:

Silicon strip detectors (single sided, each layer is rotated by 90 degrees with respect to the previous one).

Multiple scattering in the heavy material used for conversion limits the angular resolution

Calorimeter (CsI scintillator bars):

Measure the **energy** and help in reconstruction

✓8.5 radiation lengths

✓Hodoscopic (position from comparison of both ends)

✓Shower profile reconstruction (leakage correction)

Tracker Details

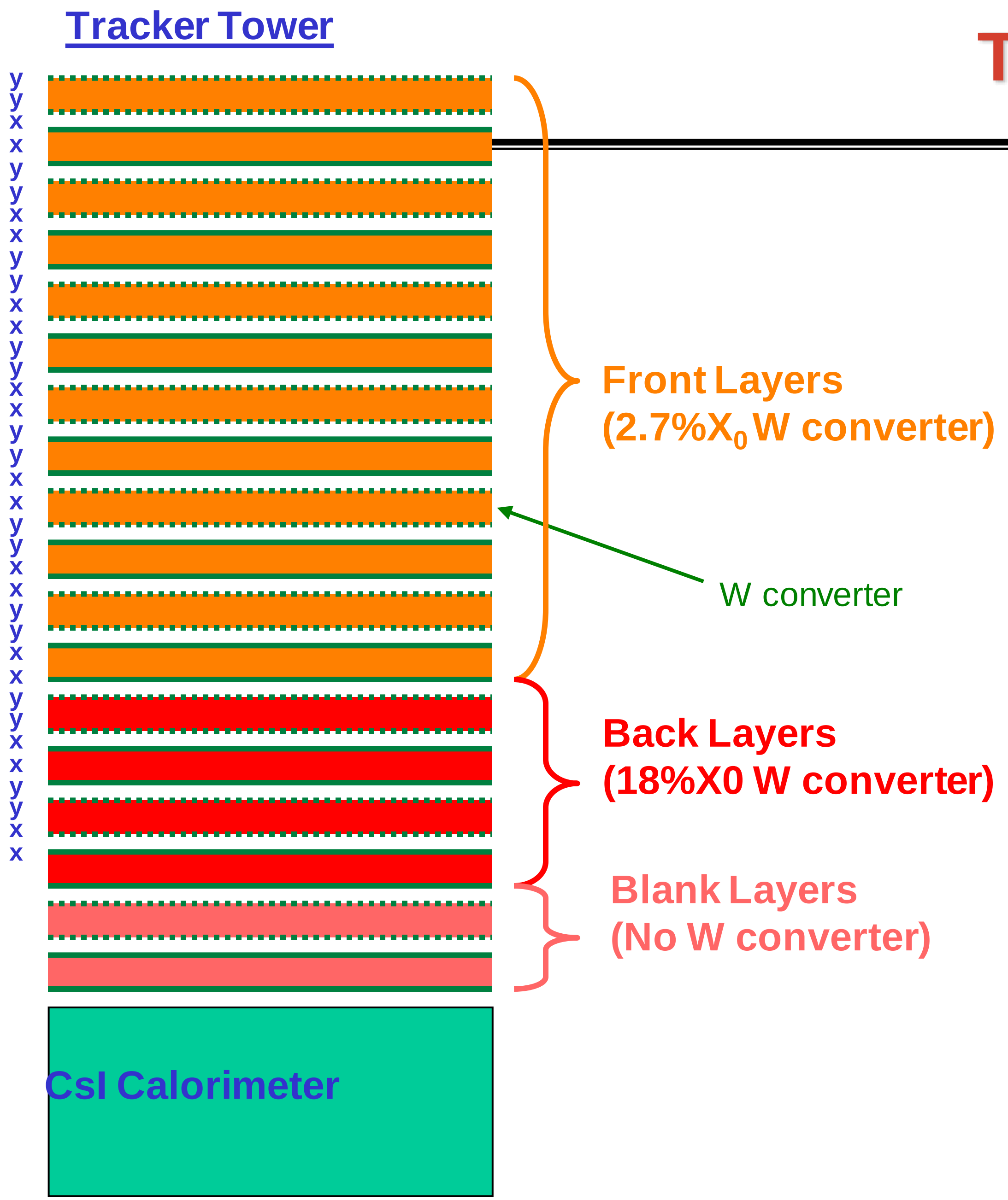

Angular resolution is determined by:
multiple scattering (at low energies) ➔ many **thin** layers
position resolution (at high energies) ➔ **fine pitch detectors**

- ❑ **Front (thin)** conversion layers to have small multiple scattering errors at low energies
- ❑ **Back** (thick) layers to increase conversion probability

Atwood *et al.* 2009, ApJ 697, 1071

Event reconstruction

27 GeV photon simulation

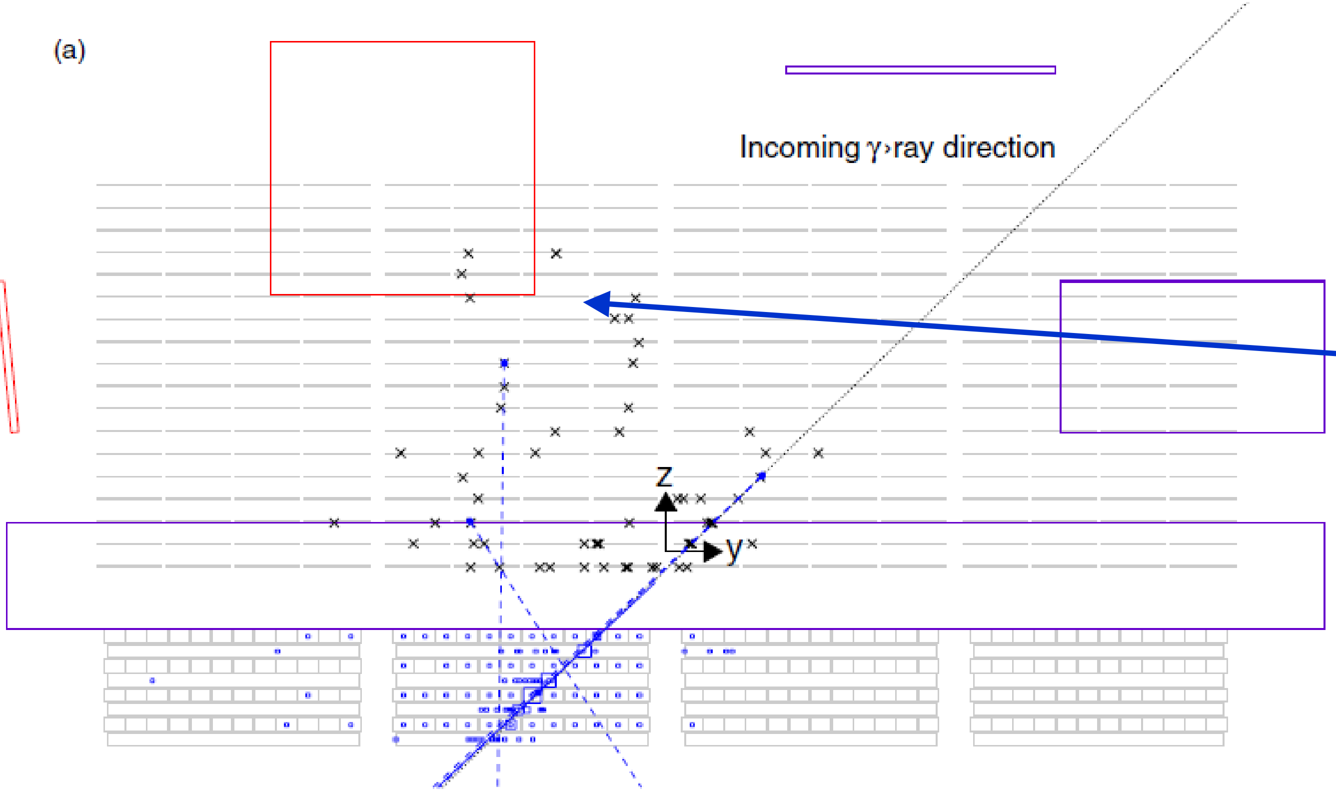

Ackermann *et al.* 2012, ApJS 203, 4

A lot on information from:

- ❑ all **points** where charged particles cross the Si strips
- ❑ all **energy deposits** in the calorimeter

High-energy showers can be very complex, with **backsplash** from the CAL into the TKR and the ACD

Requiring **two tracks** is efficient at low energy

Above 1 GeV the tracks are too close and cannot be distinguished

Event reconstruction

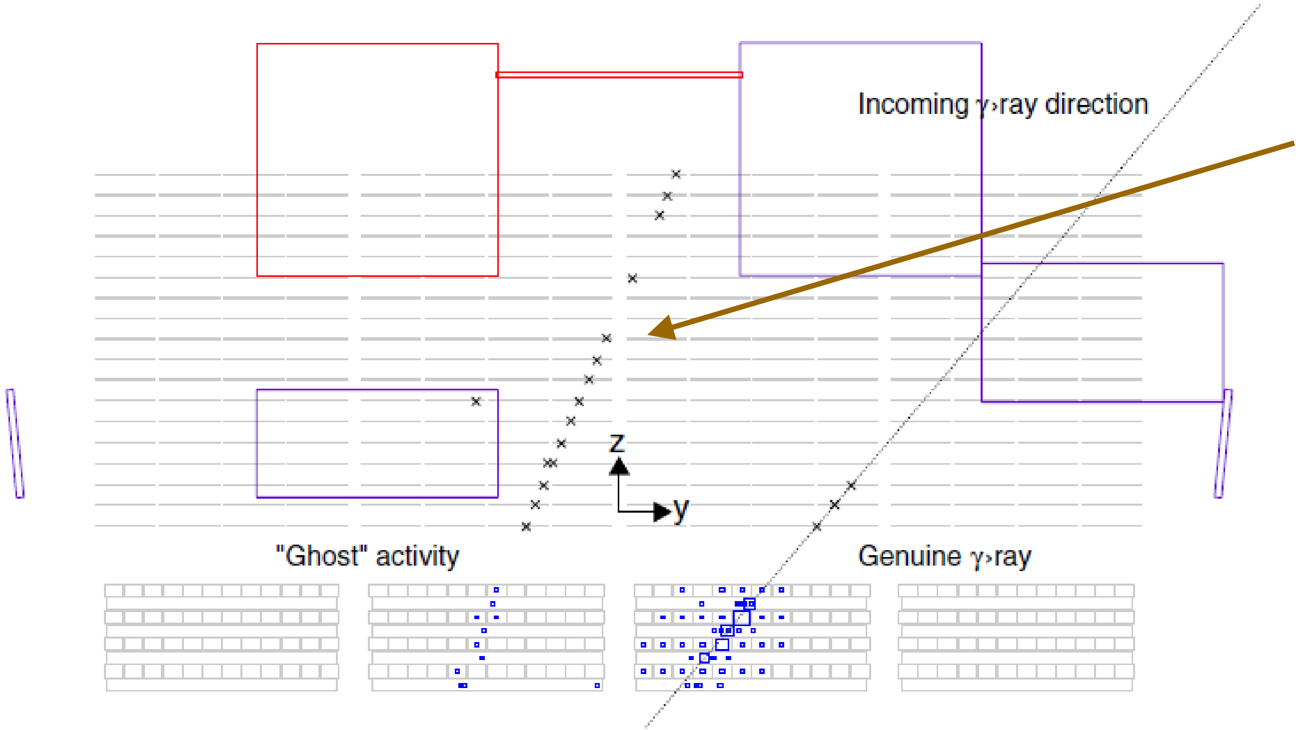

Ackermann *et al.* 2012, ApJS 203, 4

Off-time particles in the detector leave **ghost signal**

- Between 2% and 15% of the time depending on magnetic latitude (CR rate)
- Confuse/slow tracking and pattern recognition
- Must be separated during reconstruction

Events go into a **classification tree** to further reject background

Can define different **classes** (more background but more effective area)

Instrument simulation and calibration

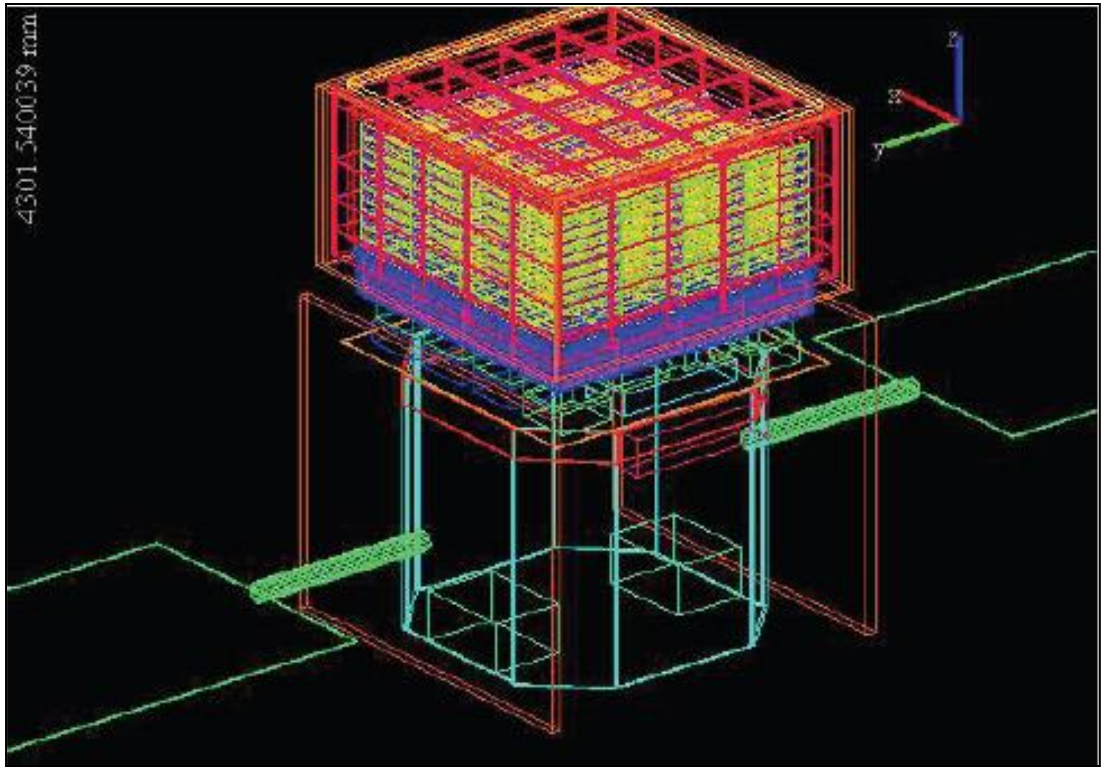

- Accurate detector model
  - > 45 k volumes
- Physical interactions modeled with **Geant4**
- Monte Carlo validation
  - ground test with CR muons on full LAT
  - beam test on a calibration unit
    - 100 M evts of g, e, p, e+, C, Xe between 50 MeV and 300 GeV collected at CERN and GSI in 2006

Calibration is **critical** to validate the simulation and event reconstruction

Point Spread Function

LAT performance page

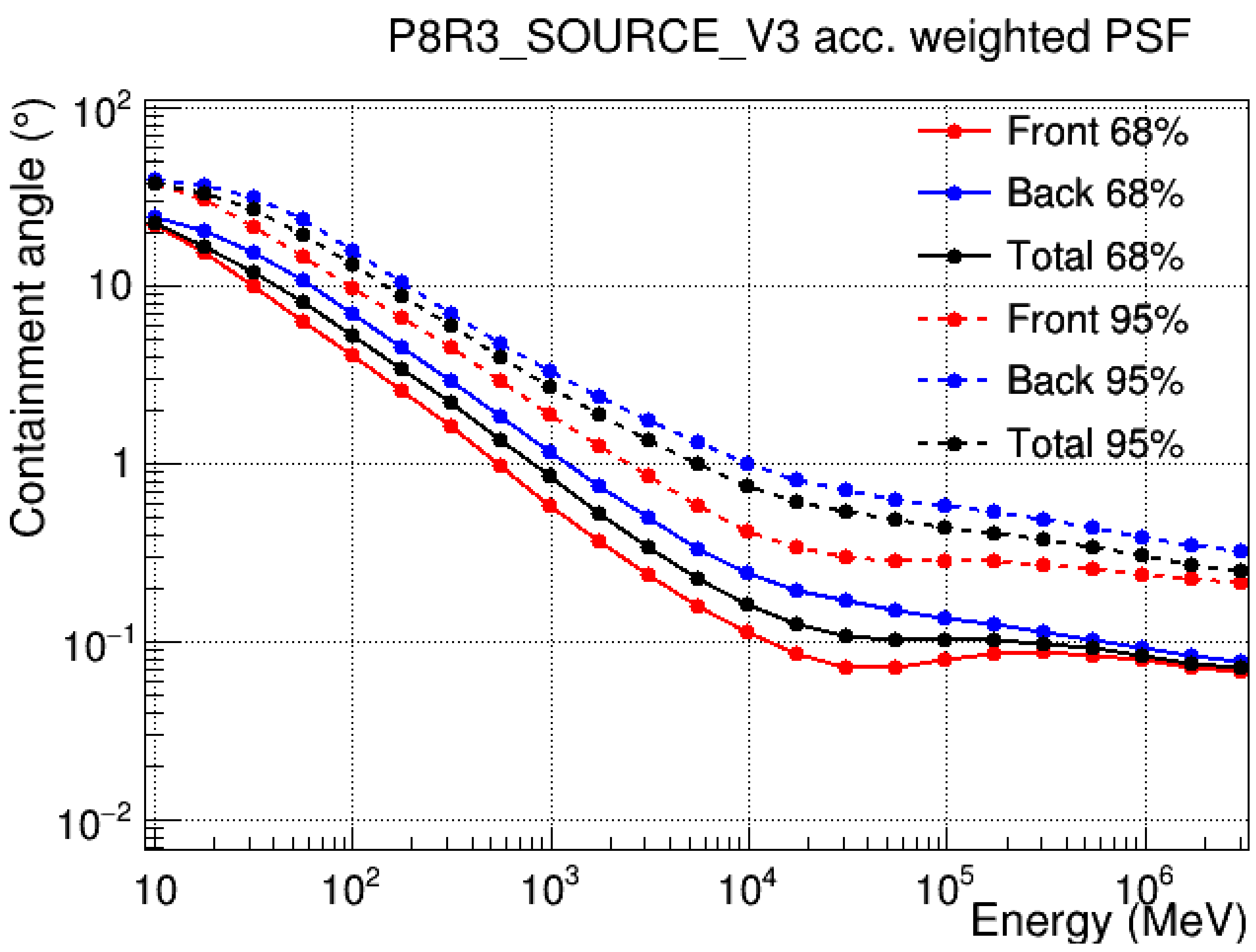

- Better PSF for Front events converted in the thin W layers
- About **twice worse** in thick (Back) layers
- Very strong **energy dependence** as $E^{-0.8}$ below 10 GeV
- Close to 0.1° (68%) above 10 GeV
- Average distance between sources is 1.4° (outside the Gal plane) ➔ **confusion** below 1 GeV

Point Spread Function

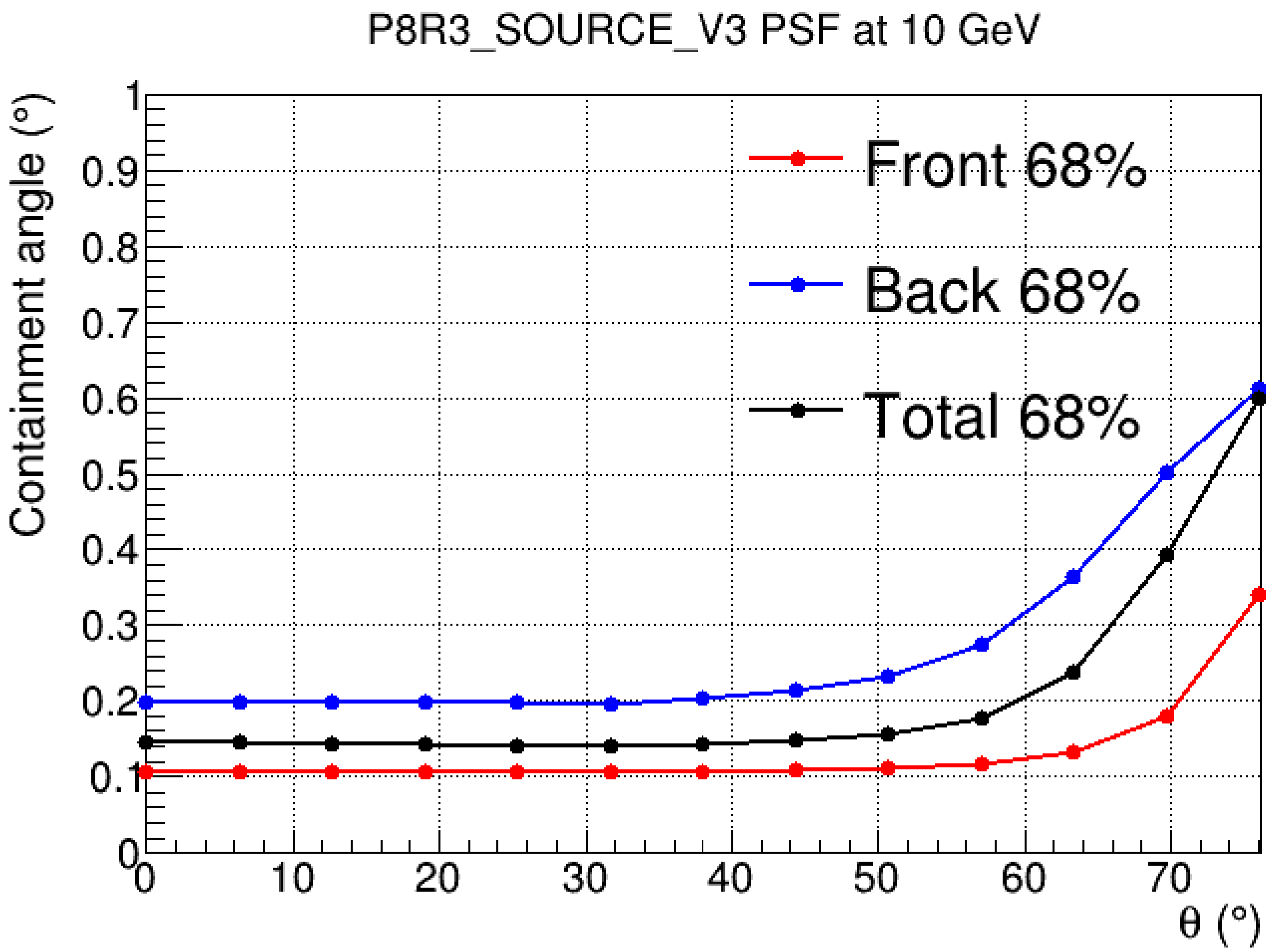

- Nearly constant up to 45° (55°) off axis for Back (Front) events
- Increases steeply further off

Point Spread Function

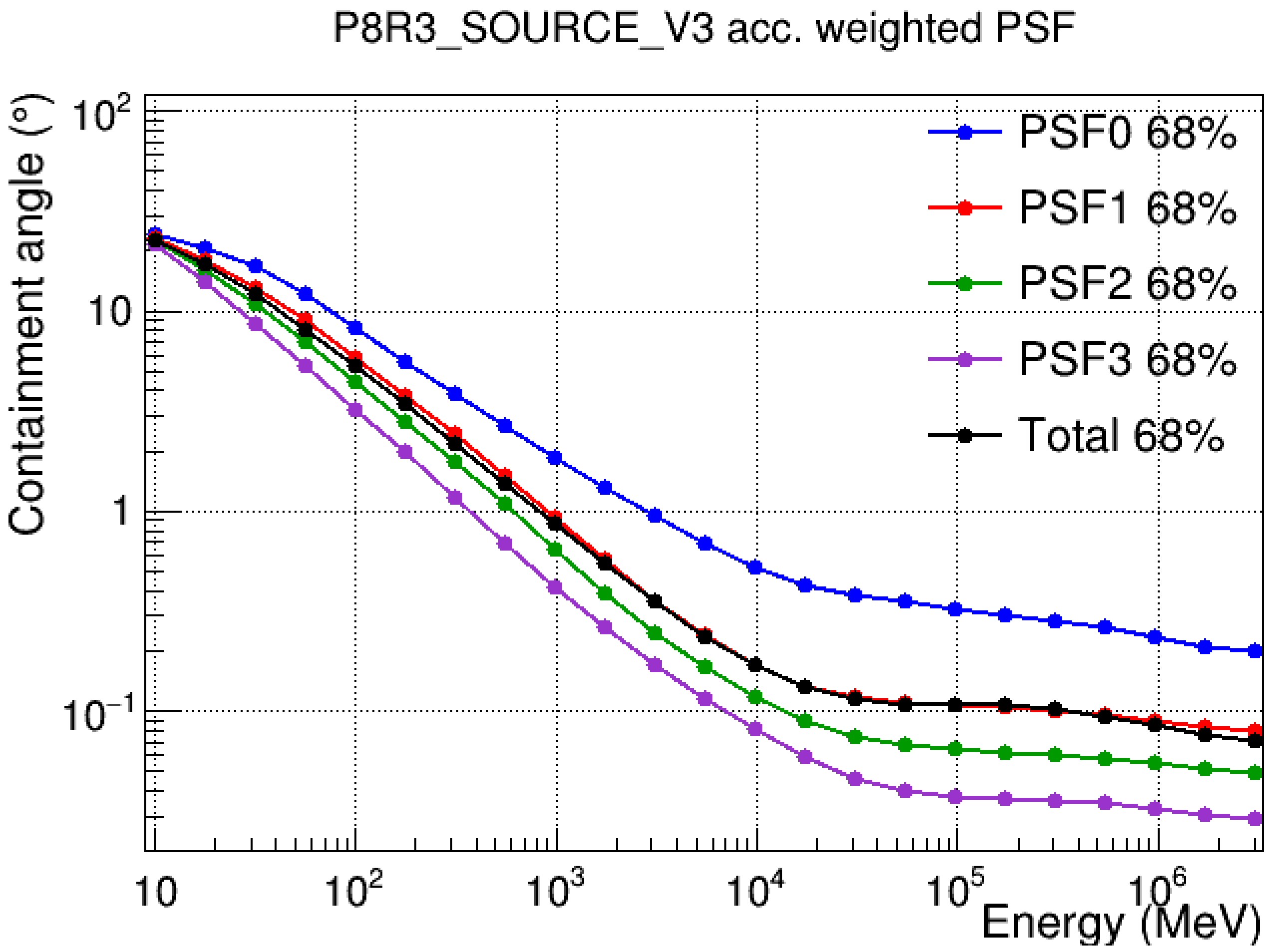

- Reconstruction allows estimating the quality of the PSF for **each event** depending on the track characteristics
- Can split events into four quasi-equal categories
- Best one (PSF3, 1/4 events) reaches < 0.05° (3 arcmin) above 20 GeV and is also better at low energies (0.4° at 1 GeV, **less confusion**)

Acceptance

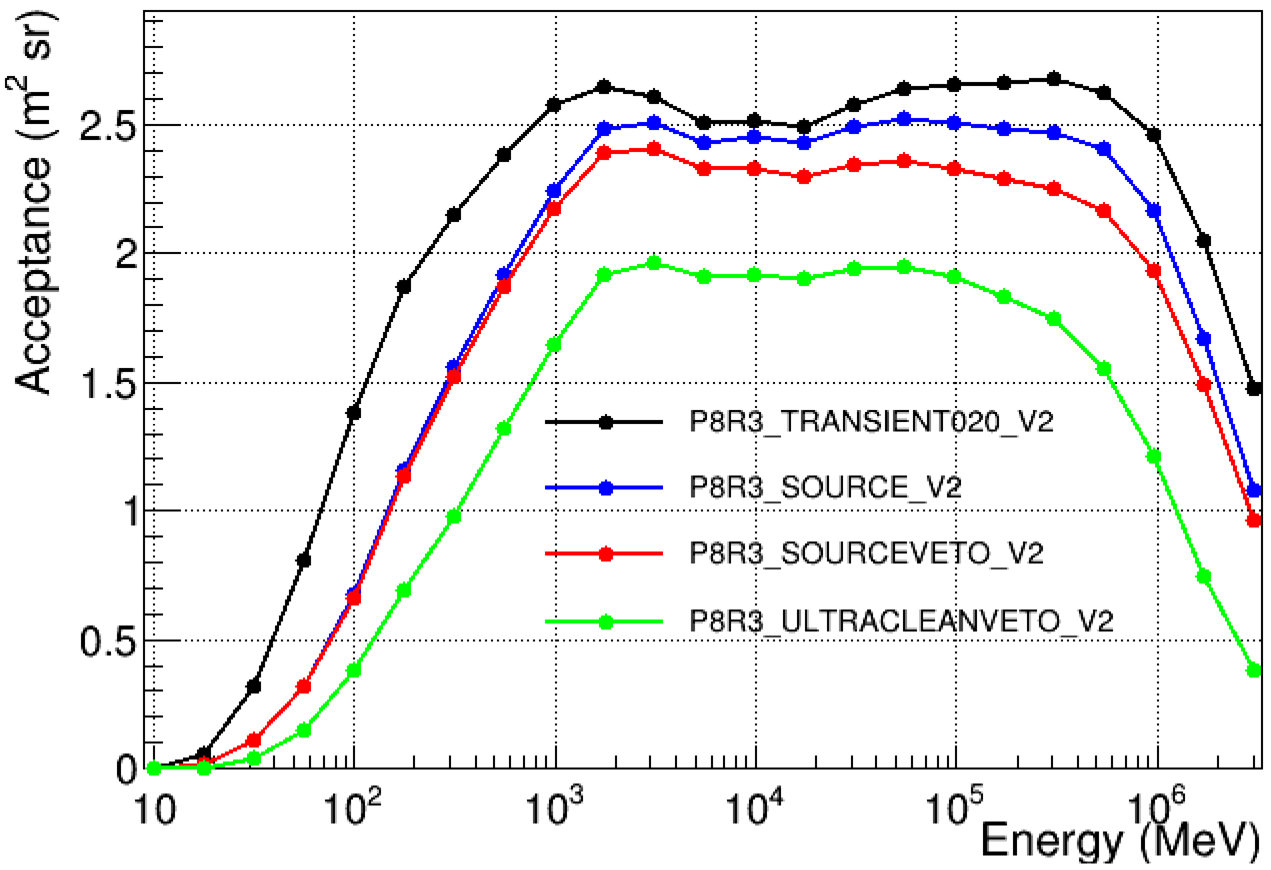

- **Acceptance** = effective area integrated over solid angle in the FOV. Relevant for surveys
- Above 2 m^2 sr between 1 GeV and 1 TeV
- Decreases steeply below 1 GeV, but that range is dominated by **background systematics** anyway
- Different event **classes** for improving instrumental background rejection

Energy resolution

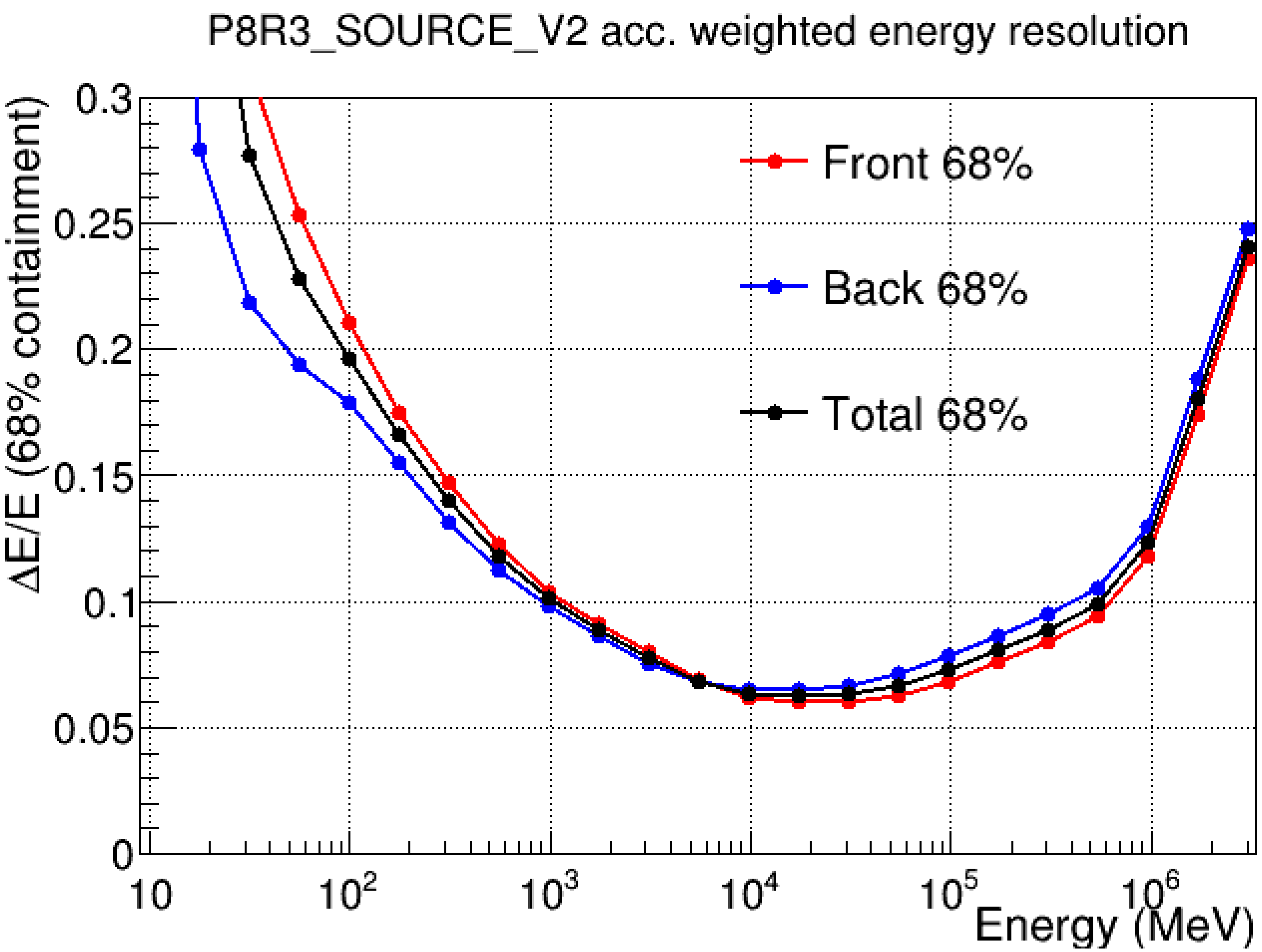

- ❑ About 10% between 1 GeV and 1 TeV
- ❑ Degrades steeply below 1 GeV, where a significant energy fraction goes into the tracker
- ❑ No strong dependence on event type

Detection threshold

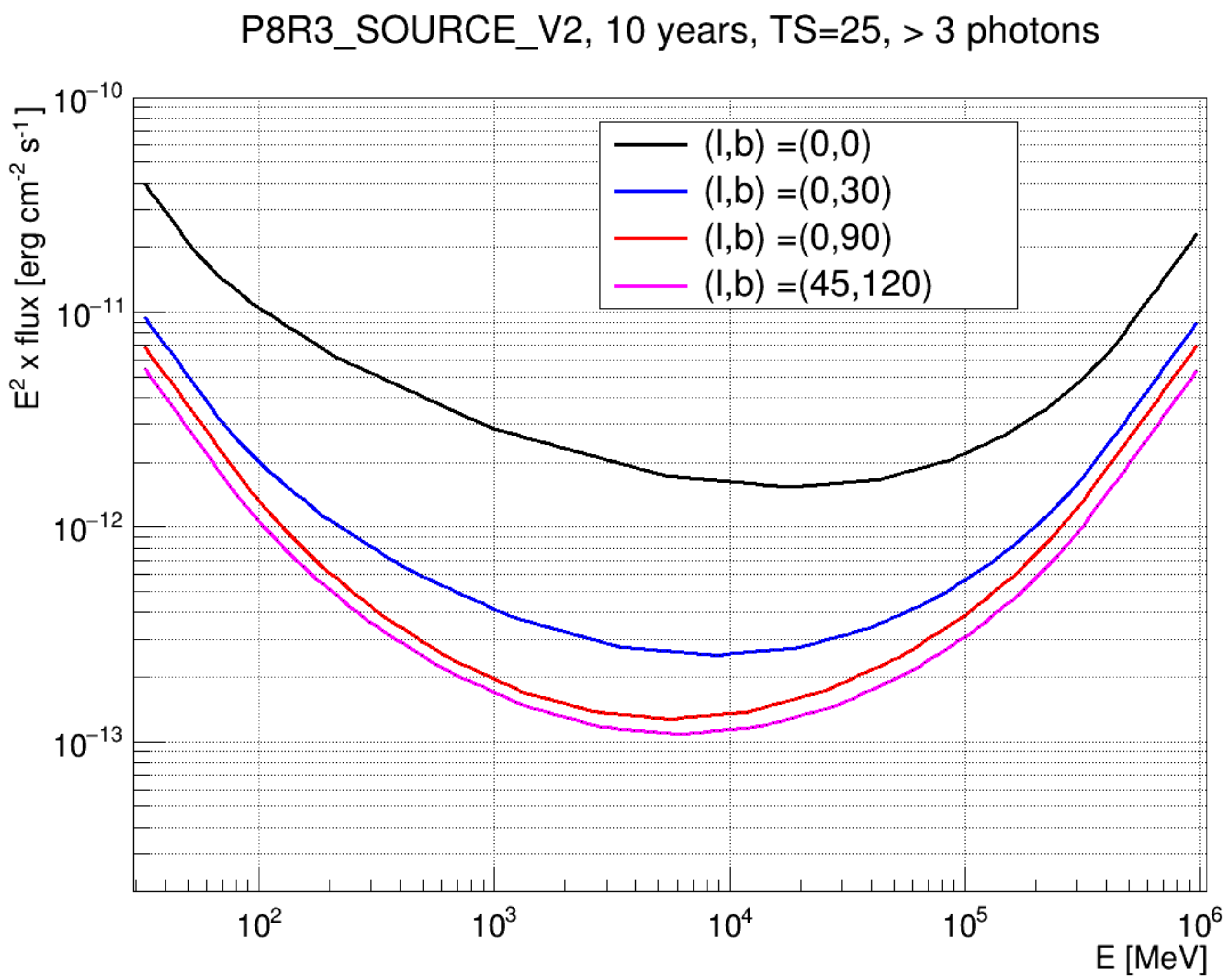

- Plotted in ***νFν* (equal energy per decade)** but the photon flux per decade decreases as 1/*E*
- For power-law spectra (envelope)
- Limited by **background** and **systematics** at low energies
- Much **worse in the Galactic plane**, particularly the Galactic Ridge (|l| < 60°) up to Cygnus and Vela
- Limited by counts at high energies

Earth albedo

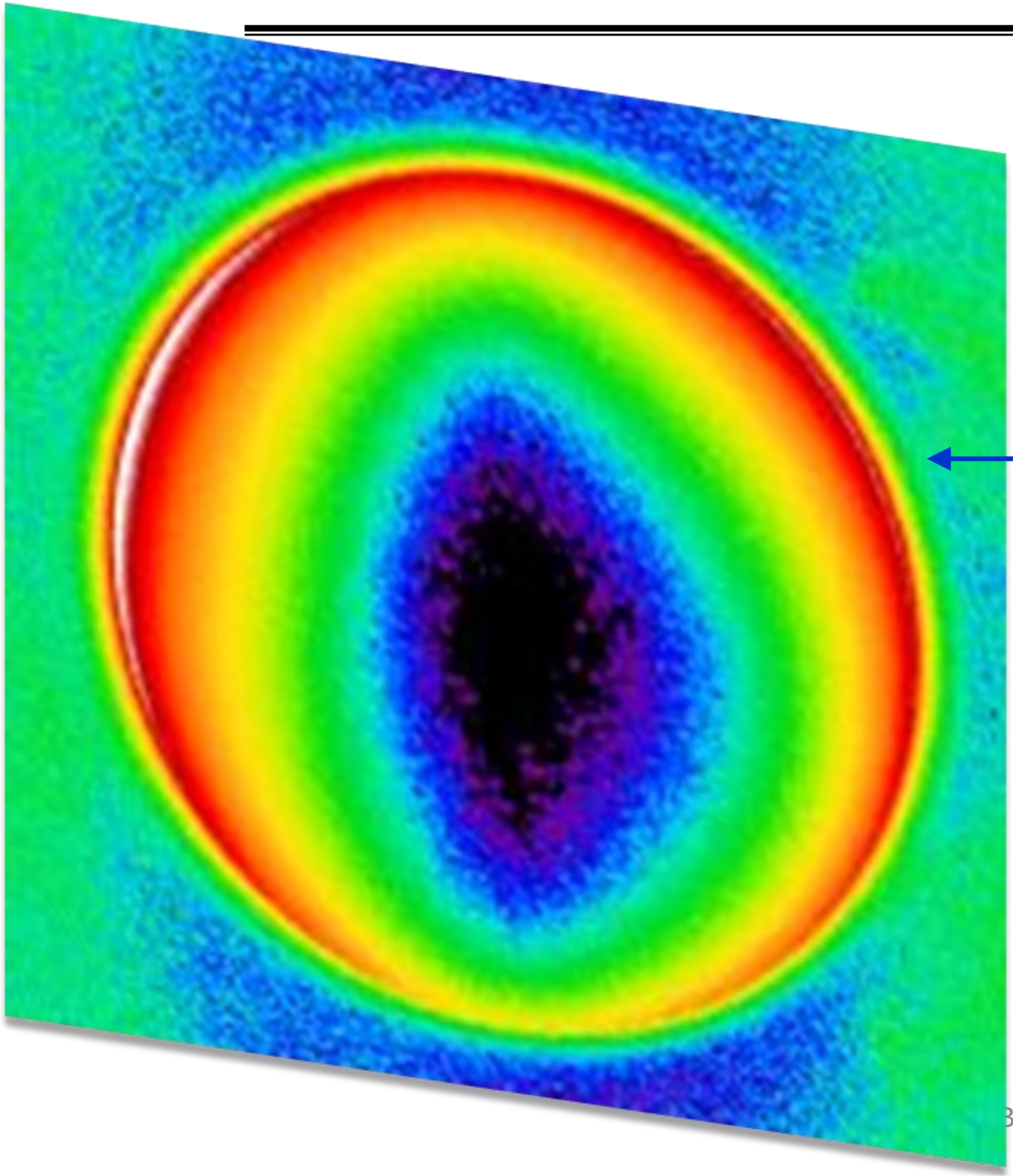

The Earth atmosphere is the strongest source of gamma rays in the Fermi range

Due to interstellar cosmic rays hitting it from outside, followed by neutral pion decay

Photon projection in **Earth coordinates** shows a very bright ring at the **Earth limb**

Strong background, must be avoided when projecting in sky coordinates

Covering the sky

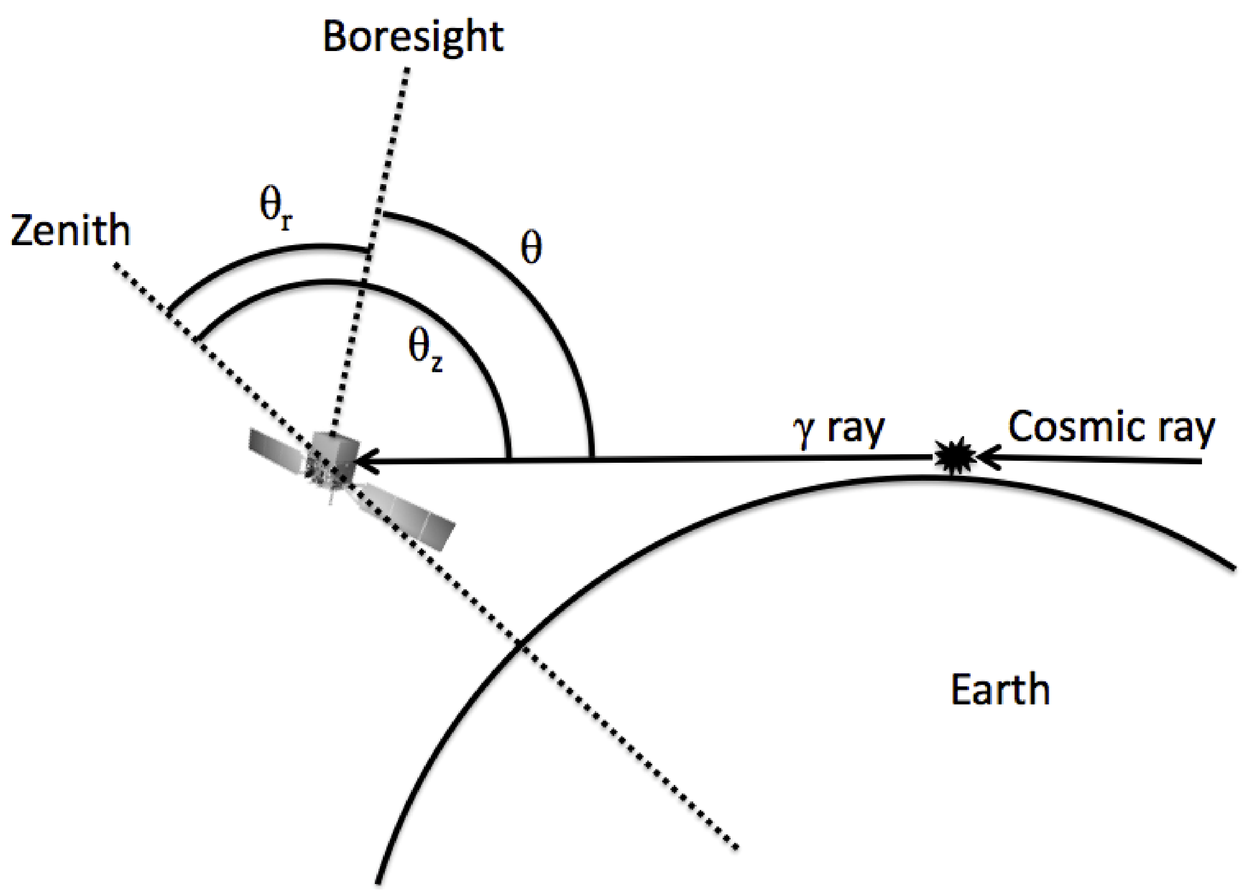

- The FOV of the LAT looks like a **cone of opening angle 60°**
- To cover the full sky, the axis is **tilted from the zenith** by θ_r = 50° transverse to the orbit, avoiding Earth limb
- The direction of this tilt is changed at every orbit (« rocking ») to cover the full sky every 3 hours
- The orbit precesses and turns around the Earth in 53.4 days, so that the sky is **covered nearly uniformly** after 2 months
- Adapted after 2018 because one solar panel is blocked

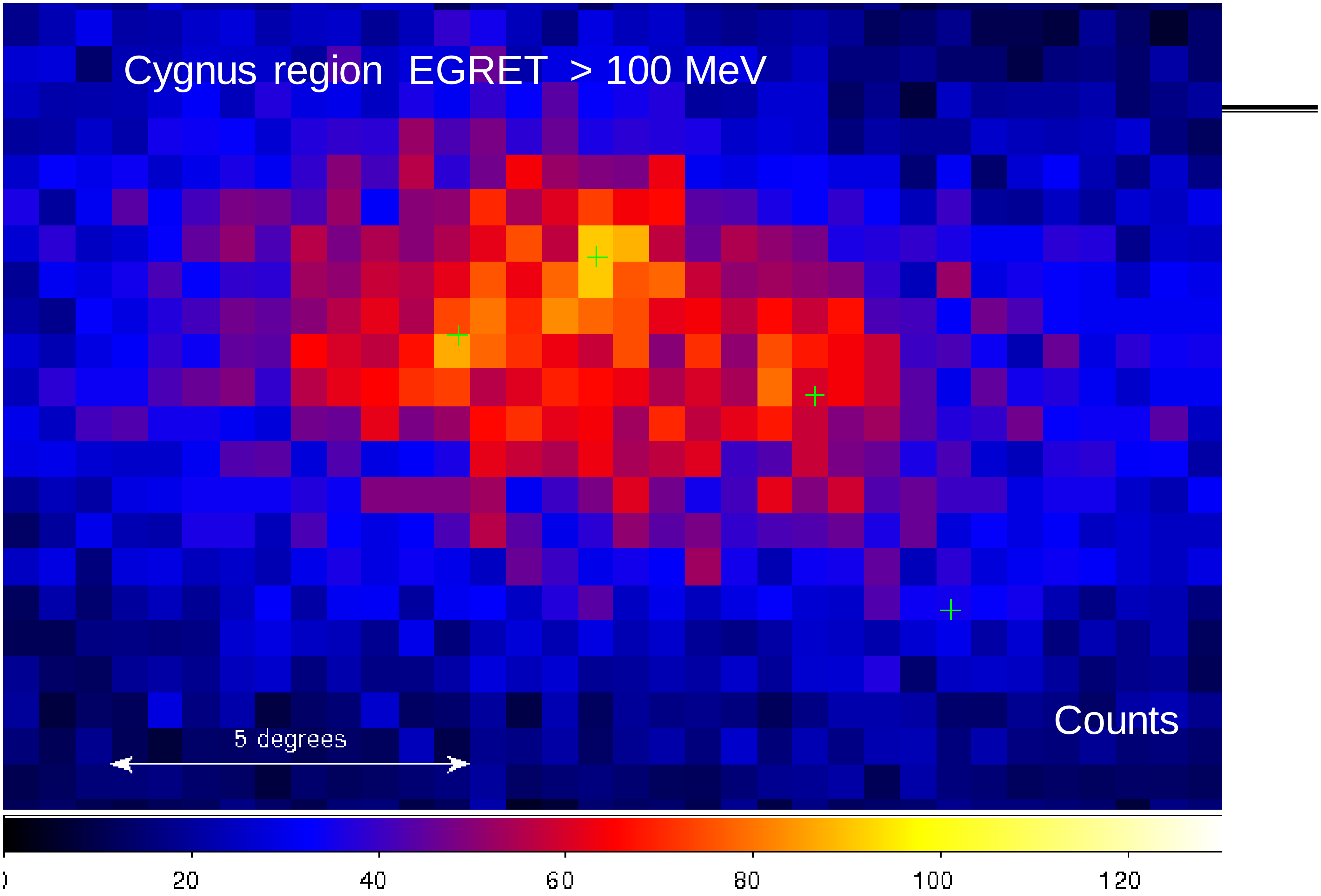
Cygnus region EGRET > 100 MeV
5 degrees
Counts
20
40
60
80
100
120

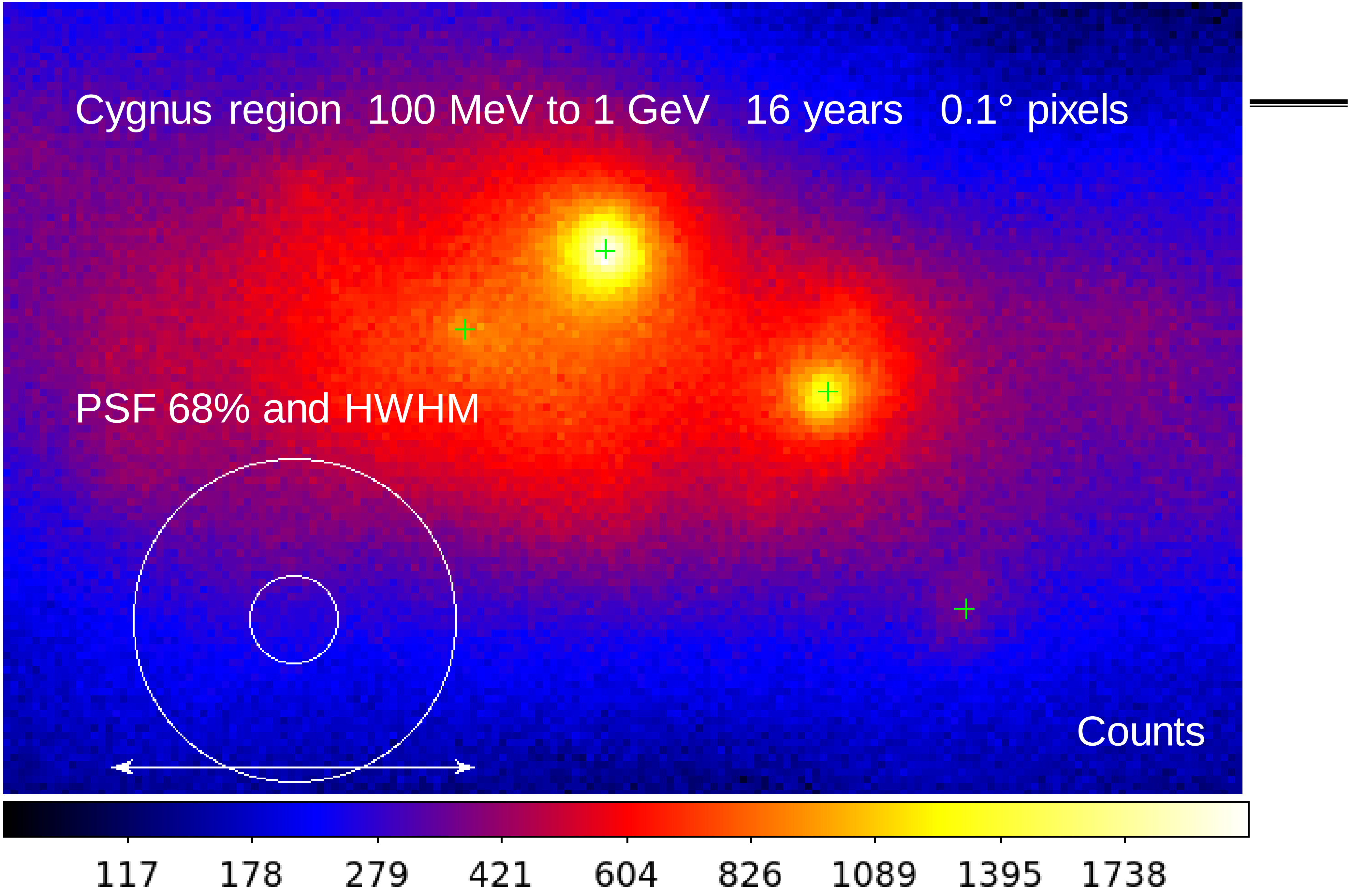

Cygnus region 100 MeV to 1 GeV 16 years 0.1° pixels
PSF 68% and HWHM
Counts
117
178
279
421
604
826
1089
1395
1738

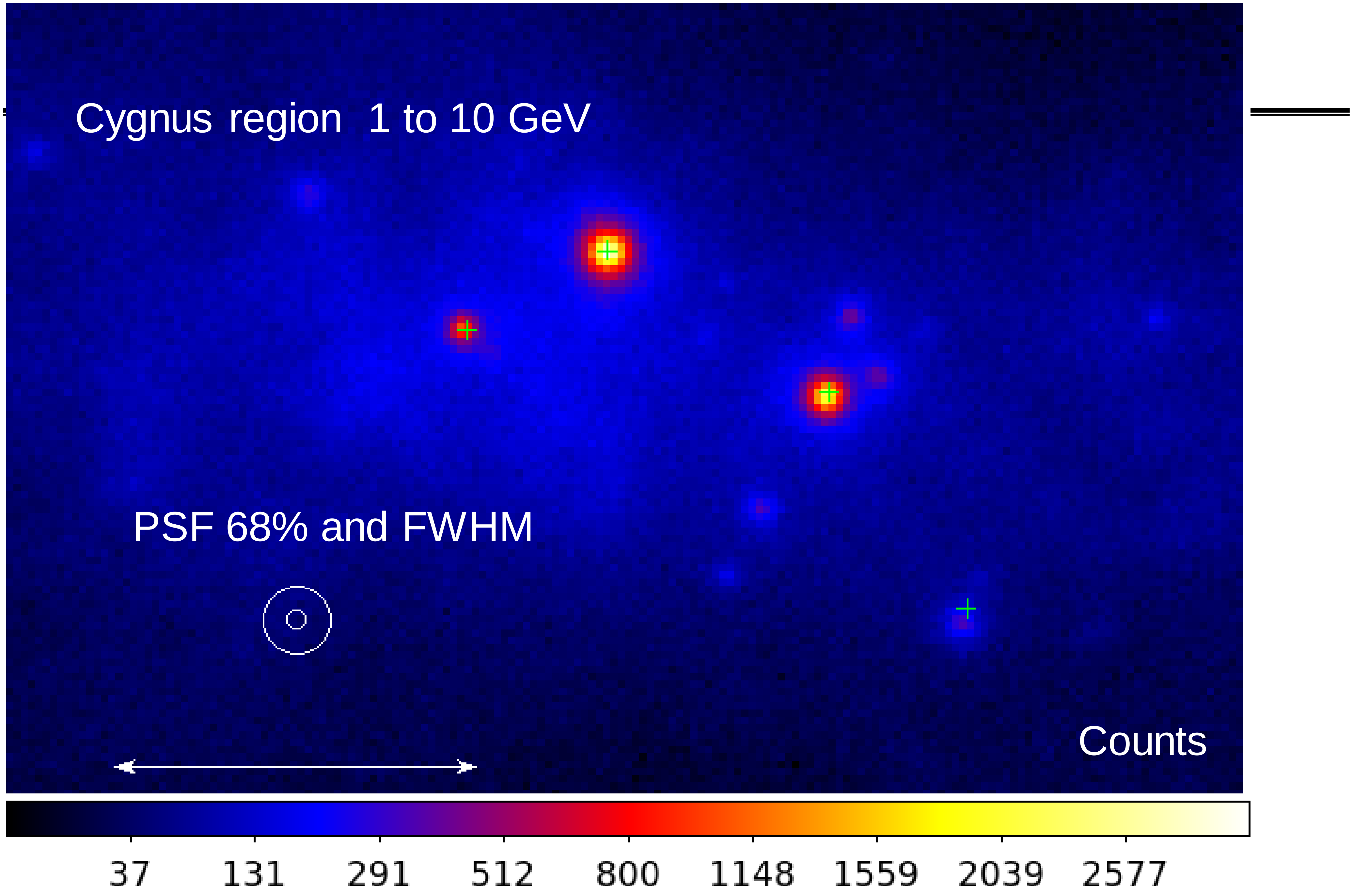

Cygnus region 1 to 10 GeV
PSF 68% and FWHM
Counts
37
131
291
512
800
1148
1559
2039
2577

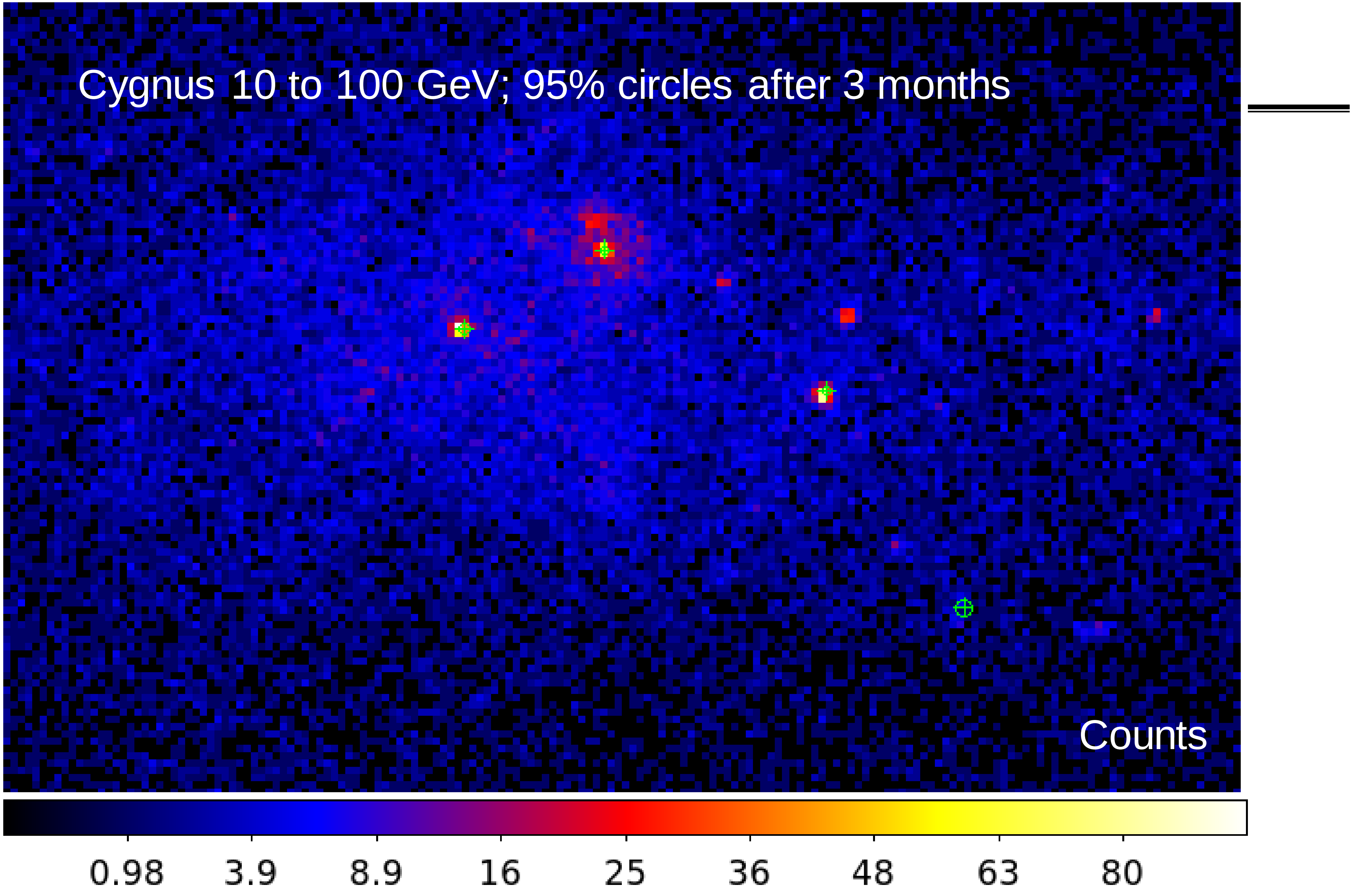
Cygnus 10 to 100 GeV; 95% circles after 3 months
Counts
0.98
3.9
8.9
16
25
36
48
63
80

Data analysis

- Strong **overlap** between sources and diffuse emission below 1 GeV
- **3D maximum likelihood** analysis (position and energy) to extract spectra from counts n_i and model M_i over all pixels i with weights w_i

$$\ln L = \sum_i w_i (n_i \ln M_i - M_i)$$

- Weights allow damping low-energy events that are dominated by **systematic uncertainties** on the interstellar emission
- Typically done over large regions (> 10°) to contain the low-energy PSF
- **Localization** anchored at highest energies

Comparison to ground Cherenkov detectors

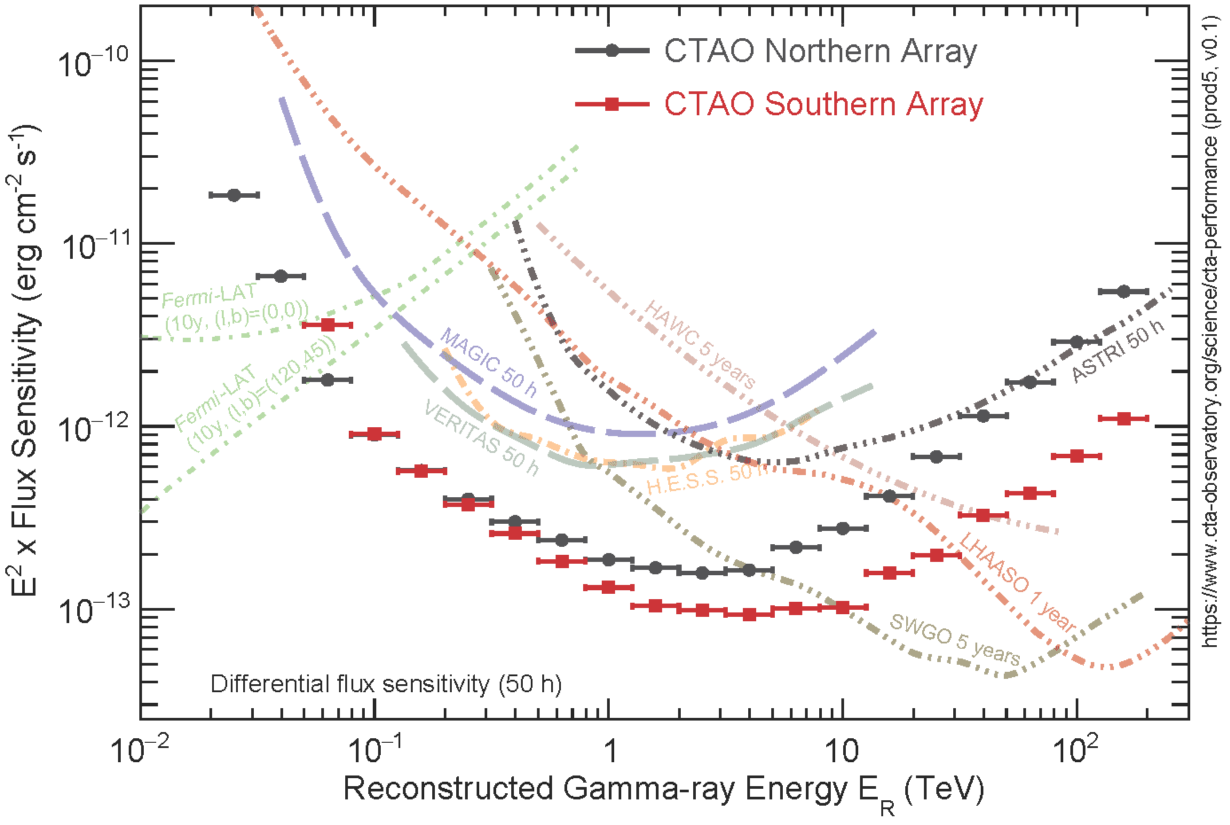

- ❑ Space detectors can never be made as big as IACTs (HESS, VERITAS, MAGIC)
- ❑ But they **observe quasi permanently** so they reach a comparable sensitivity after several years
- ❑ They are more comparable to water Cherenkov detectors (HAWC, LHAASO WCDA)
- ❑ **Complementarity**: detailed study for IACTs, average properties with space detector or water Cherenkov
- ❑ Space detectors are in the **photon-limited** regime above 10 GeV where sensitivity improves nearly as 1/T rather than 1/√T

Outlook

- Below 1 MeV, the **transient sky** (GRBs and flares) is adequately covered (Fermi-GBM, Swift-BAT, SVOM-ECLAIRs)
- In the **MeV range**, COSI will help but it is too small to bridge the gap between the hard X-ray (NuSTAR) and GeV ranges
  ➔ this remains the **least well covered** energy range
- The **GeV range** is **well covered** by Fermi-LAT, the future could be HERD on the Chinese space station